DESIGN AND IMPLEMENTATION OF A HIGH-SPEED INVERSE WALSH TRANSFORM APPARATUS

DESIGN AND IMPLEMENTATION OF A HIGH-SPEED INVERSE WALSH TRANSFORM APPARATUS

by

SAMIA R. MIKHAIL, B.Sc. (AIN SHAMS UNIV., EGYPT)

A Thesis

Submitted to the School of Graduate Studies

in Partial Fulfilment of the Requirements

for the Degree

Master of Engineering

McMaster University

May 1972

MASTER OF ENGINEERING (1972)
(Electrical Engineering)

McMASTER UNIVERSITY
Hamilton, Ontario

TITLE: Design and Implementation of a High-Speed Inverse Walsh Transform Apparatus

AUTHOR: Samia R. Mikhail, B.Sc., Ain Shams University, Cairo, Egypt

SUPERVISOR: Professor A. R. Elliott

NUMBER OF PAGES: 73, viii

SCOPE AND CONTENTS:

In this thesis, a high-speed inverse Walsh transform apparatus was designed and built which sums over the sixteen most dominant coefficients in the time base period. The transform includes a maximum of 64 terms. The Walsh function generator used works with a clock rate up to 10 MHz to produce 64 different sequency terms with accurate timing and hazard free operation. A synchronizing pulse is produced by the circuit to determine the beginning of the Walsh transform period. The final adder stage limits the speed of the apparatus to a 1 MHz square wave. An application of the instrument was made to reconstruct one line of an actual video signal.

ACKNOWLEDGEMENTS

The author is greatly thankful to Dr. A. R. Elliott for his assistance and valuable suggestions during the course of this work. The author also wishes to express her appreciation to Mr. M. Beshai for his help in preparing the computer program. The author would like to thank Mrs. Rita Gibson for typing of the thesis.

TABLE OF CONTENTS

		Page
CHAPTER I:	INTRODUCTION ----------------------------------	1
CHAPTER II:	MATHEMATICAL BASICS ------------------------	4
	2.1 The Walsh Functions --------------------	5
	2.2 Series Expansion by Walsh Function ------	12
	2.3 Amplitude Sampling and Walsh Fourier Analysis	14
	2.4 Fast Walsh Fourier Transform ------------	15
CHAPTER III:	CIRCUIT DESIGN FOR AN INVERSE WALSH TRANSFORM INSTRUMENT -----------------------------------	18
	3.1 The Walsh Function Generator -----------	22
	3.2 The Multiplier -------------------------	34
	3.3 The Adder ------------------------------	38
	3.4 Testing of the Instrument --------------	41
CHAPTER IV:	INSTRUMENT APPLICATION ON A VIDEO SIGNAL -----	44
	4.1 The Video Signal ----------------------	45
	4.2 A Walsh Transform for the Video Signal --	45
	4.3 The Instrument Application -------------	48
	4.4 The Two Dimensional Walsh Fourier Transform	50
CHAPTER V:	CIRCUIT DESIGN ERRORS AND LIMITATION ---------	54
	5.1 Mathematical Error ---------------------	54
	5.2 Circuitry Error -----------------------	55

		Page
CHAPTER VI:	CONCLUSIONS --------------------------------	57
APPENDICES	---	58
APPENDIX A	WALSH TRANSFORM FOR SPECIFIC SIGNALS --------	59
APPENDIX B	LAYOUT OF CIRCUIT BOARDS -------------------	67
REFERENCES	---	72

LIST OF ILLUSTRATIONS

FIGURE		Page
1	The Walsh Function Generator	6
2	The Radmacher Functions	8
3	Fast Walsh Transform for 8 Data Points	16
4	The Generalized Transform Coding	19
5	The Inverse Walsh Transform Circuit	21
6	Walsh Function Generator as Product of Radmacher Functions	23
7	The Rate Multiplier	25
8	The Output State of a 3 Bit Rate Multiplier	27
9	The Flip-Flop Output Toggled by the Possible Output From 3 Bit Rate Multiplier	28
10	The Walsh Function Generator	30
11	Simultaneous Generation of Walsh Functions with the Same Counter	31
12	Schematic of Walsh Function Generator Card 1 or Card 2	33
13	Analog Multiplication By ±1	35
14	Multiplier Circuit	36
15	Circuit for the Coefficient a_i	39
16	One Step Adder	39
17	Schematic Diagram of Multipliers and Summer Card 1 and Card 2	40
18	Reconstruction of Known Signals by the Designed Instrument	42

FIGURE		Page

19	The Composite Video Signal According to United States Standard ----------------------------	46
20	An Actual Video Signal ----------------------------	49
21	Reconstruction of the Video Signal, for 64 Samples in the Transform Period -------------------	51
22	Reconstruction of 32 Samples of the Video Signal --	52
B-1	The Walsh Function Generator Card 1 or Card 2 -----	68
B-2	The Multipliers and Summer Card 1 ----------------	69
B-3	The Multipliers and Summer Card 2 ----------------	70
B-4	The Integrated Circuits --------------------------	71

LIST OF TABLES

TABLE		Page
I	The Ordered Walsh Functions as Product of Radmacher Functions --	9
II	Walsh Function Determination by Knowing the Sequence ----	12
A-1	The Walsh Transform of a Sinusoidal Signal --------------	60
A-2	The Walsh Transform of a Ramp Signal --------------------	61
A-3	The Walsh Transform of a Triangle Signal ----------------	61
A-4	A Typical Video Signal (Fig. 20(b), 256 samples in the period T) ---	
A-5	The Walsh Transform for 64 Successive Samples of the Video Signal --	63
A-6	The Walsh Transform for 32 Samples of the Video Signal --	65

CHAPTER I

INTRODUCTION

Recently, a set of orthogonal functions known as the Walsh functions has received great interest in the communications field[1-9]. Since they are a two level set, they are directly compatible with digital circuitry and digital computers. They appear to be as ideal for linear, time variable circuits, if based on binary digital components, as the system of trigonometric functions is for linear, time-invariant circuits, based on resistors, capacitors and coils. Their practical application, however, will require considerable progress in the development of large scale integrated circuits.

In this thesis, the idea of transmitting the information content of a wide band signal by the Walsh-Fourier transform is used. This may lead to a bandwidth reduction for image transmission in digital communication systems. At the transmitter, the Walsh transform of the signal could be obtained, quantized, and coded for transmission. At the receiver, the information must go through an inverse transform to obtain the reconstructed signal. This double transformation, once at the transmitter and once at the receiver, will be discussed throughout this report as the double Walsh transform.

A high speed inverse Walsh transform instrument has been implemented for this work, which consists of Walsh function generators, multipliers and a summer. This transform design proceeds in parallel and in analog form to obtain high speed operation. A similar instrument by Brown[2] uses digital circuitry and serial arithmetic to perform the inverse transform. The Walsh function generator is able to generate up to 64 different sequency terms in the unit period of time chosen as a time base for the Walsh functions. The function is generated according to a standard binary code for the Walsh number. A synchronizing pulse is produced at the beginning of the time period. This circuit is hazard free with no timing error. By the use of high speed logic the circuit worked up to 10 MHz. The additional circuit is analog in nature using IC analog multipliers. The summation is made over a set of 16 coefficients of the transform using a standard operational amplifier adder. This adder limits the speed of the apparatus to about a 1 MHz square wave.

An application of the designed instrument was made on an actual video signal. A Walsh transform was obtained for the signal by computer simulation. The sixteen most dominant coefficients were fed to the inverse Walsh transform apparatus. The output from the apparatus gave the double Walsh transformed signal within certain error.

The next chapter clarifies the mathematical basics of the work in this thesis. The Walsh functions and associated properties are defined. The conversion of a time series to a Walsh series is shown and a fast Walsh transform for the conversion is explained.

In Chapter III the inverse Walsh transform instrument design is described. The instrument is tested for reconstruction of some known signals. The following chapter describes the application of the apparatus on the video signal. The reconstructed signal is shown for different time base periods of the transform.

The errors of the circuit design are discussed in Chapter V. The final chapter is a conclusion about the work done and future research in this subject.

CHAPTER II

MATHEMATICAL BASICS

Data compression techniques have been used in many areas of communications, such as voice, video and telemetry transmission to reduce the bandwidth needed to transmit a given amount of information in a given time. Such compressions must be accomplished without sacrificing the information requirements of the user. The reduction in the bandwidth required for any signal transmission is achieved by reducing signal redundancy. Shannon has defined the redundancy as "that fraction of a message or datum which is unnecessary and hence repetitive in the sense that if it were missing, the message would still be essentially complete or at least could be completed"[10].

Data compression techniques are classified into many categories. One classification is known as the transformation compression technique[11]. This is defined as any compression technique which transforms either analog or digital data by a linear or nonlinear transformation. An inverse transform must be performed at the receiving end to reconstruct the original data. Signal conditioners, filters, limiters/clippers and spectrum analysers are examples of transformation compression.

The type of transformation compression considered in this work is the Walsh Fourier transform and its application to video signals. The Walsh transform is a square array of plus and minus ones whose rows and columns are orthogonal to one another. The time required to obtain the

Walsh transform of a signal is drastically reduced by using the fast Walsh transform method. This is a high speed algorithm similar to the fast Fourier transform, but is a faster operation since only real number additions and subtractions are required for a Walsh transformation rather than a complex multiplication as in the fast Fourier transform case.

2.1 THE WALSH FUNCTIONS:

The Walsh functions have received considerable interest in the communications field lately[1-9]. They are a set of functions that are periodic and orthogonal. The complete set can be defined by Wal(i,θ) as given by Harmuth[3], where i represents the number of sign changes of the function in the unit period of θ. The Walsh functions can also be represented by a constant Wal(0, θ), even functions Cal(i, θ) and odd functions Sal(i, θ) in analogy to the even and odd trigonometric functions cos θ and sin θ, such as:

$$\begin{aligned} \mathrm{Cal}(i, \theta) &= \mathrm{Wal}(2i, \theta) \\ \mathrm{Sal}(i, \theta) &= \mathrm{Wal}(2i-1, \theta) \end{aligned} \tag{1}$$

Figure 1 shows the first 16 functions of Wal(i, θ) in the normalized interval θ = 1, where θ = t/T and T is the time base for the Walsh function. These functions are switching between two values, +1 and -1, all having the value +1 at θ = 0. Also, Wal(0, θ) is a constant with value +1. The functions are arranged in the order of their sequency which is defined as "1/2 the average number of zero crossing per unit interval of time"[3] for which the abbreviation 'ZPS' is used. This is an order principle which maintains the analogy to the frequency of circular functions.

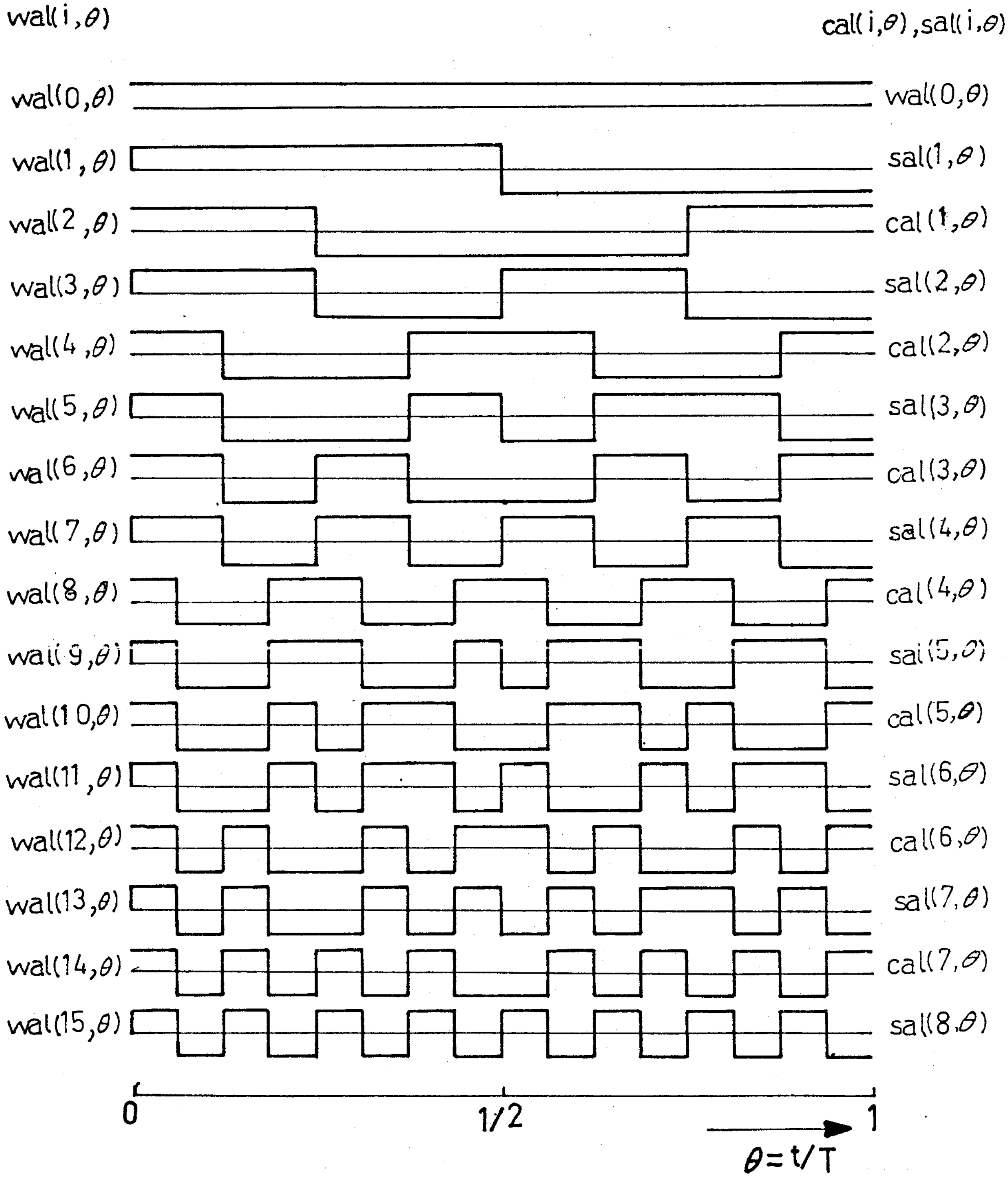

FIGURE 1: The Walsh Functions

Another way of defining the Walsh functions is by using Radmacher functions $R_n(\theta)$[4], which are a subgroup of the complete Walsh set, such that:

$$R_n(\theta) = Wal(2^{n-1}, \theta) \qquad n = 1,2,\ldots \qquad (2)$$

The Radmacher functions are square waves. The first four $R_n(\theta)$ are shown in Figure 2, and they are defined as follows:

$$R_o(\theta) \equiv 1$$

$$R_n(\theta) = 1 \quad \text{if } \frac{2k}{2^n} \leqslant \theta < \frac{(2k+1)}{2^n}$$

$$= -1 \quad \text{if } \frac{(2k+1)}{2^n} \leqslant \theta < \frac{(2k+2)}{2^n} \qquad \text{---- (3)}$$

$$k = 0, 1, 2, \ldots, 2^{n-1}-1$$

The Walsh functions can be produced by all the possible Boolean products of the Radmacher functions. From the first n Radmacher functions, N Walsh functions can be generated (where $N = 2^n$). This produces a complete and orthogonal set of functions. Therefore:

$$Wal(0, \theta) \equiv 1$$

$$Wal(n, \theta) = R_{n_1+1} \, R_{n_2+1} \, \ldots\ldots \, R_{n_r+1}$$

$$n = 2^{n_1} + 2^{n_2} + \ldots\ldots + 2^{n_r} \qquad \text{---- (4)}$$

where $n_1 > \ldots > n_r \geqslant 0$

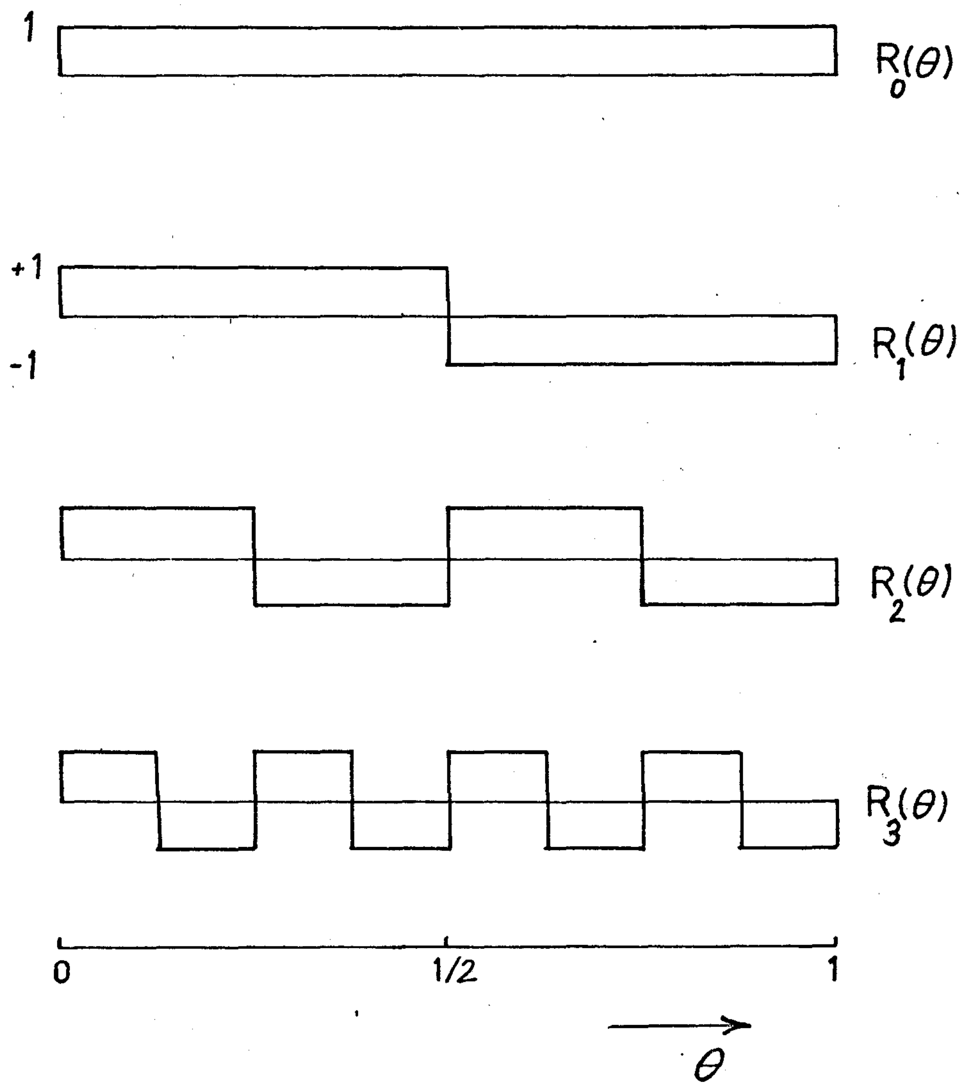

FIGURE 2: Radmacher Functions $R_n(\theta)$

However, this definition does not lead to the set of Walsh functions ordered by their sequency. The correct Radmacher functions to multiply together to obtain a specified Walsh function can be determined by reference to a reflected binary code (Gray code). This method is shown in Table I up to $n = 3$. The rows correspond to the W_i and the columns numbered from right to left to R_j. The 1's in any row indicate the R_j whose direct product is the W_i on that row.

	R_3	R_2	R_1
W(0, θ) 000			
W(1, θ) 001			1
W(2, θ) 010		1	1
W(3, θ) 011		1	
W(4, θ) 100	1	1	
W(5, θ) 110	1	1	1
W(6, θ) 110	1		1
W(7, θ) 111	1		

TABLE I: The Ordered Walsh Functions as Product of Radmacher Functions

The main property of the set of Walsh functions is the multiplication property, which states that: the product of two Walsh functions yields another Walsh function[3].

$$Wal(i, \theta).Wal(k, \theta) = Wal(i \oplus k, \theta) \quad (5)$$

where $\oplus$ stands for addition modulo 2 in binary representation, i.e., $0 \oplus 1 = 1 \oplus 0 = 1, 0 \oplus 0 = 1 \oplus 1 = 0$. This property is the way for the conversion from Radmacher function to the ordered Walsh function as given in Table I, since Equation (5) can be written as:

$$W_g = R_h W_{2^n-1-g} \quad (6)$$

where $g = 2^{h-1}, 2^{h-1} + 1, \ldots, 2^h-1$

and $g = 1, 2, \ldots, n$

This implies that for the first 2^n rows of a matrix of Walsh functions, any W_g in the lower half of that set of rows is different from the one symmetrically located in the upper half with respect to a horizontal centre line (i.e., W_{2^h-1-g}) only by the presence of R_h. This is precisely a description of the reflected binary code of n variables.

Another property[7] of the Walsh function set $Wal(i,\theta)$ is that it is symmetrical with respect to the argument i, θ. By interchanging these two variables the same system will give the values of all the orders of Walsh functions at a given time. This property is written as:

$$Wal(i, \theta) = Wal(\theta, i) \quad (7)$$

This property shows the symmetry of the Walsh matrix.

The orthogonality of the Walsh functions in the normalized interval $0 \leq \theta < 1$ is given by the following condition:

$$\int_0^1 Wal(i, \theta)\, Wal(j, \theta)\, d\theta = \delta_{ij} \tag{8}$$

$$\delta_{ij} = 1 \quad \text{for} \quad i = j \quad , \quad \delta_{ij} = 0 \quad \text{for} \quad i \neq j$$

This condition can be proved directly from the multiplication property (5) noting that:

$$Wal(i, \theta)\, Wal(i, \theta) = Wal(0, \theta)$$

$$Wal(i, \theta)\, Wal(0, \theta) = Wal(i, \theta)$$

There is a simple way to determine the Walsh function of any order at sight, without using a previously computed function, by symmetry considerations.[9] For any Walsh function Wal(i, θ) where i corresponds to the number of zero crossings in the unit interval of θ, i can be written in binary form as:

$$i = 2^k + a_{k-1}\, 2^{k-1} + \ldots + a_1 2 + a_o$$

where a_j is either 0 or 1. Wal(i, θ) is symmetric or skew symmetric about θ = 1/2 according to a_o = 0 or 1. This gives the even and odd Walsh functions Cal(i, θ), and Sal(i, θ). This symmetry consideration can be extended to determine Wal(i, θ) completely. By dividing the interval θ = 1 into 2^{k+1} subintervals of length $2^{-(k+1)}$, then Wal(i, θ) is symmetric or skew symmetric about $\theta = 1/2^{j+1}$ according as a_j = 0 or 1 for j = k, k-1, ..., 1, 0. Letting Wal(i, θ) = 1 in the first interval ($0 \leq \theta < 2^{-k+1}$), the Walsh function Wal(i, θ) can be determined by knowing the sequence i only. A demonstration for determining the first 8 Walsh functions using this method is given in Table II.

vertical image axes

$W_{a_2a_1a_0}$		a_2	a_1		a_0			
W_{000}	+	+	+	+	+	+	+	+
W_{001}	+	+	+	+	-	-	-	-
W_{010}	+	+	-	-	-	-	+	+
W_{011}	+	+	-	-	+	+	-	-
W_{100}	+	-	-	+	+	-	-	+
W_{101}	+	-	-	+	-	+	+	-
W_{110}	+	-	+	-	-	+	-	+
W_{111}	+	-	+	-	+	-	+	-

$0 \quad \frac{1}{8} \quad \frac{1}{4} \quad \frac{1}{2} \quad 1$

$\longrightarrow \theta$

TABLE II: Walsh Function Determination by Knowing the Sequence

2.2 SERIES EXPANSION BY WALSH FUNCTIONS:

Any periodic time function f(t) quadratically integrable in the interval $t_o < t < t_o + T$ for which $\int_{t_o}^{t_o+T} f^2(t)dt < \infty$, can be expanded in a series of the orthonormal system of Walsh functions Wal(i, θ) in the interval of orthogonality $0 \leq \theta < 1$, where $\theta = (t - t_o)/T$. The expansion of f(t) will be given as:

$$f(\theta) = \sum_{i=0}^{\infty} a_i \, \mathrm{Wal}(i, \theta) \tag{9}$$

The coefficients a_i of the series expansion can be obtained by multiplying Equation (9) by Wal(j, θ) and integrating the result over the period of orthogonality $0 \leq \theta < 1$ using the orthogonality relation (8). Therefore,

$$a_i = \int_0^1 f(\theta)\ \mathrm{Wal}(i, \theta)d\theta \tag{10}$$

The series expansion of f(θ) can be expressed in terms of the even and odd Walsh functions Cal(i, θ), Sal(i, θ) as:

$$f(\theta) = a_0 + \sum_{i=1}^{\infty} [a_i\ \mathrm{Cal}(i,\theta) + b_i\ \mathrm{Sal}(i,\theta)] \tag{11}$$

where $$a_0 = \int_0^1 f(\theta)d\theta$$

$$a_i = \int_0^1 f(\theta)\ \mathrm{Cal}(i,\theta)d\theta \tag{12}$$

$$b_i = \int_0^1 f(\theta)\ \mathrm{Sal}(i,\theta)d\theta$$

A Walsh transform for the signal f(θ) can be obtained as with the Fourier transform by stretching the interval θ, and considering f(θ) to be zero outside the original period of orthogonality. In the limit as $\theta \rightarrow \pm\ \infty$ the Walsh transform will be given by:

$$a_\mu = \int_{-\infty}^{\infty} f(\theta)\ \mathrm{Wal}(\mu,\theta)d\theta$$

and (13)

$$f(\theta) = \sum_{\mu=0}^{\infty} a_\mu\ \mathrm{Wal}(\mu,\theta)d\mu$$

2.3 AMPLITUDE SAMPLING AND WALSH FOURIER ANALYSIS:

The sampling theorem as applied to Fourier analysis states that a signal, band limited to B Hz is completely determined by 2B amplitude samples per second. This theory holds true too for the Walsh Fourier analysis. A simple proof is shown in the following paragraph.

Let a signal f(t) band limited to B Hz be represented by amplitude samples taken at a rate of 2B samples per second. If we take a period T as a time base for a Walsh function such that $2BT = 2^n = N$ equal to the number of samples in this time interval, and making $\theta = t/T$, then the expansion of the signal f(t) in the normalized Walsh series will be:

$$f(\theta) = \sum_{i=0}^{\infty} a_i \, Wal(i,\theta) \qquad 0 \leq \theta < 1 \tag{14}$$

The coefficients a_i are given by Equation (10) (repeated here) as:

$$a_i = \int_0^1 f(\theta) \, Wal(i,\theta) d\theta \tag{15}$$

From the skew symmetry property of Walsh functions as demonstrated in Table II for $n = 3$, the Walsh Fourier coefficients a_i for $i \geq N$ will vanish, since each sample will be eliminated by itself, providing that the square wave representation is precisely as accurate as the sampled data. As an example, consider the case when $N = 4$. There are then four samples in the interval $0 \leq \theta < 1$. Let them be labelled S_1, S_2, S_3, and S_4. Then the coefficient for $Wal(6, \theta)$ would be obtained from (15) as:

$$a_6 = \frac{1}{4} [(S_1 - S_1) + (S_2 - S_2) - (S_3 - S_3) - (S_4 - S_4)] = 0$$

Similarly all the coefficients from a_4 to a_∞ will be zero. This means that the maximum sequency contained in the signal f(t) in the interval T is (2BT - 1) = (N - 1). This will be the upper limit in the summation of (14) instead of ∞. Hence

$$f(\theta) = \sum_{i=0}^{N-1} a_i \, \mathrm{Wal}(i,\theta) \qquad 0 \leq \theta < 1 \qquad (16)$$

In other words, the maximum sequency of the signal f(t) is B zps.

By representing $f(\theta)$ by N samples in the interval $0 \leq \theta < 1$, the integration of Equation (15) can be changed to a summation by dividing the period θ into N subintervals of length 1/N. The coefficients a_i are given by:

$$a_i = \frac{1}{N} \sum_{\theta=0}^{N-1} f(\theta) \, \mathrm{Wal}(i,\theta) \qquad i = 0, 1, \ldots N-1 \qquad (17)$$

2.4 FAST WALSH FOURIER TRANSFORM:

The fast Walsh transform, quite similar to the fast Fourier transform [7], is a highly efficient procedure for computing the Walsh transform of a time series. It takes advantages of the fact that the calculations of the coefficients of the Walsh transform can be carried out iteratively, which results in a considerable saving of computer time. The computation of the Walsh transform of a signal $f(\theta)$ as given by Eq. (17) in the straighforward method requires N^2 operations, where an operation is defined to be either an addition or subtraction. Using the fast Walsh transform algorithm, this reduces to $N \log_2 N$ operations.

Figure 3 illustrates the computation sequence performed by the fast Walsh transform with eight data samples. The samples are arranged

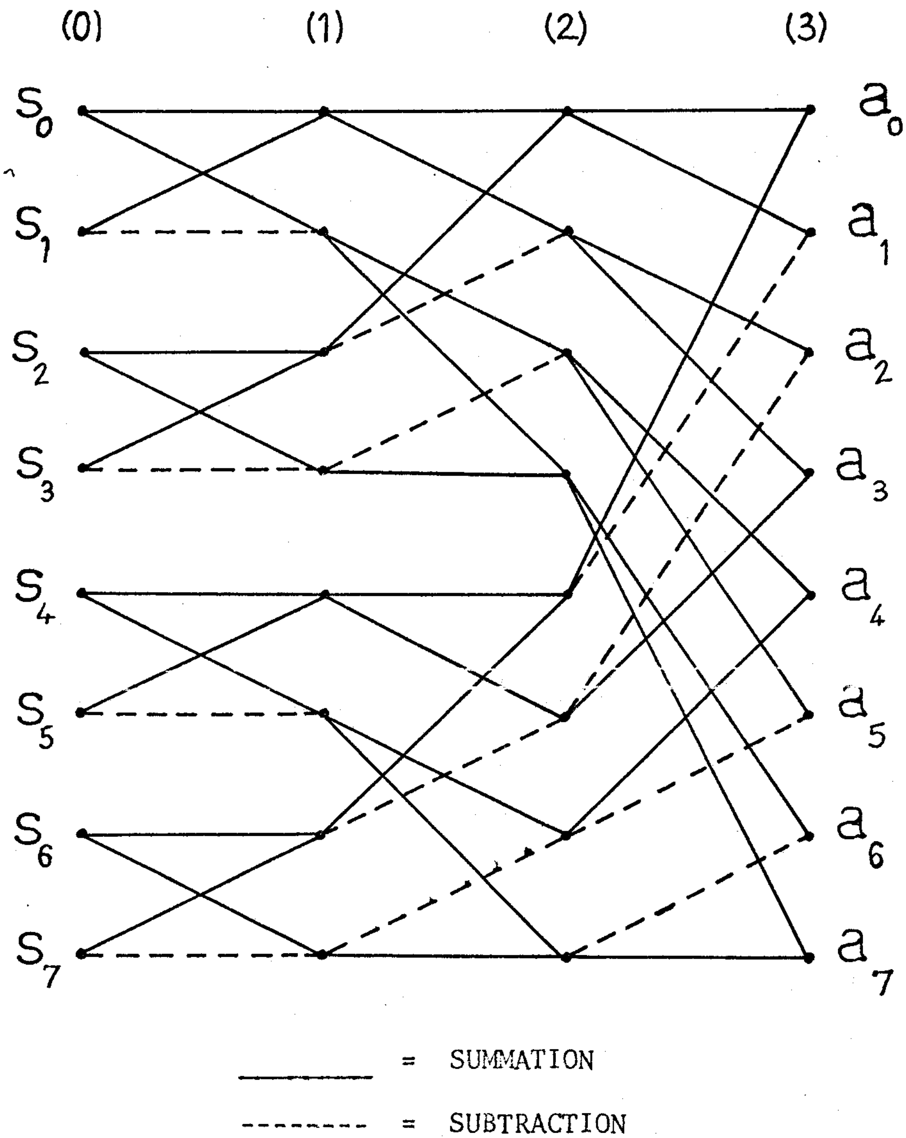

FIGURE 3: Computation of the Walsh Transform for Eight Data Points

in a column and then summed (or subtracted) by pairs to produce an intermediate result. The procedure continues until the eight Walsh coefficients are obtained after three stages. A dotted line linking two nodes indicates that the sample point forms the subtrahend of a subtraction operation. There are two operations performed at each node in the three stages yielding a total of $8 \log_2 8 = 24$ operations compared to $8 \times (8-1) = 56$ operations in the straightforward way.

A fast Walsh transform algorithm was used to obtain the Walsh transform of several signals used in this thesis.

CHAPTER III

CIRCUIT DESIGN FOR AN INVERSE WALSH TRANSFORM INSTRUMENT

The block diagram for a generalized transform coding system is shown in Figure 4. In this system, a transform is performed on the samples of the signal. The transform samples are then quantized and coded for transmission over a digital link. At the receiver, the received data is decoded and an inverse transform is performed to reconstruct the original signal.

The Walsh Fourier transform is applied in this work for wide band signal transmission system. If $N = 2^n$ is the number of samples representing the signal f(t) in the period T, then the Walsh transform of f(t) and its inverse are given by Equations (16) and (17) as:

$$f(\theta) = \sum_{i=0}^{N-1} a_i \, \mathrm{Wal}(i, \theta) \qquad 0 \leq \theta < 1 \tag{16}$$

$$a_i = \frac{1}{N} \sum_{\theta=0}^{N-1} f(\theta) \, \mathrm{Wal}(i, \theta) \qquad i=0,1,\ldots,N-1 \tag{17}$$

where $\theta = t/T$, and T is the time base for the Walsh function.
The Walsh transform a_i of f(t) was performed by a digital computer simulation using the fast Walsh transform technique. A circuit was designed to do the inverse Walsh transform on the computed data providing an analog

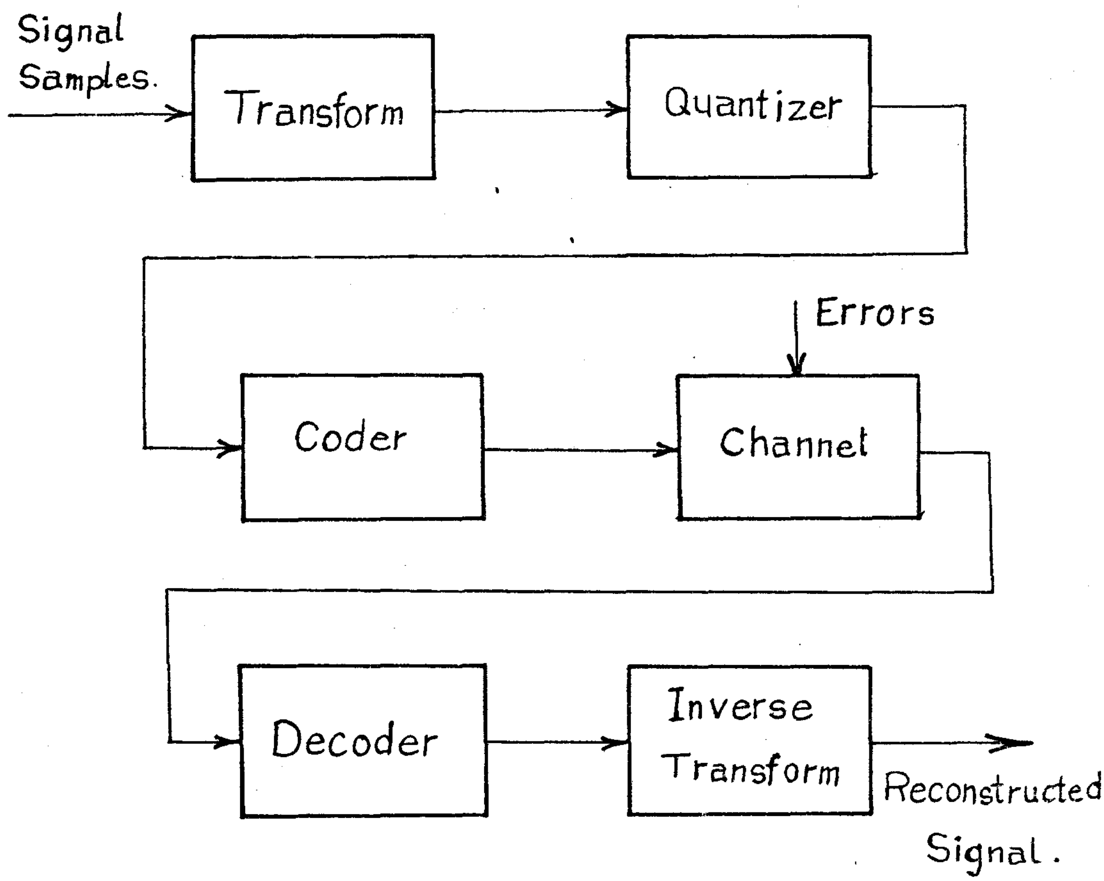

FIGURE 4: Transform Coding System

output signal $\hat{f}(t)$, which is the double Walsh transformed signal within certain error.

Figure 5 illustrates the block diagram of the circuit for the inverse transform as given by Equation (16). The input coefficient data (a_i) was converted to an analog voltage by a D/A converter, then multiplied with the corresponding Walsh function Wal(i, θ) generated from a Walsh function generator. Finally, the outputs from the multipliers (M) are summed together using the resistance R and the operational amplifier to form the signal $\hat{f}(\theta)$. The errors in this assumption for the double Walsh transformed signal are due to quantization for coding.

In the designed circuit, the inverse Walsh transform is performed by summing over only the 16 most dominant coefficients of the Walsh transform. The apparatus constructed uses an analog signal source for the coefficient a_i instead of a digital to analog converter. The maximum absolute value for the input coefficients was limited by the multipliers used in the circuit to $\approx$ 1.2 volts maximum.

The Walsh function generator is able to produce 64 different sequencies according to a standard binary code for the input sequence. In general, the input data are changing with every new period of the Walsh transform. A synchronizing pulse is produced to determine the beginning of the period θ. The multiplier that was used was an IC circuit which actually functions as a modulator. A d-c signal corresponding to the coefficient is placed on one terminal, while the Walsh function generator drives the other. The output in effect is the Walsh function amplitude moldulated by the input coefficient. Ordinary resistances R and an operational amplifier are used in a standard summing stage.

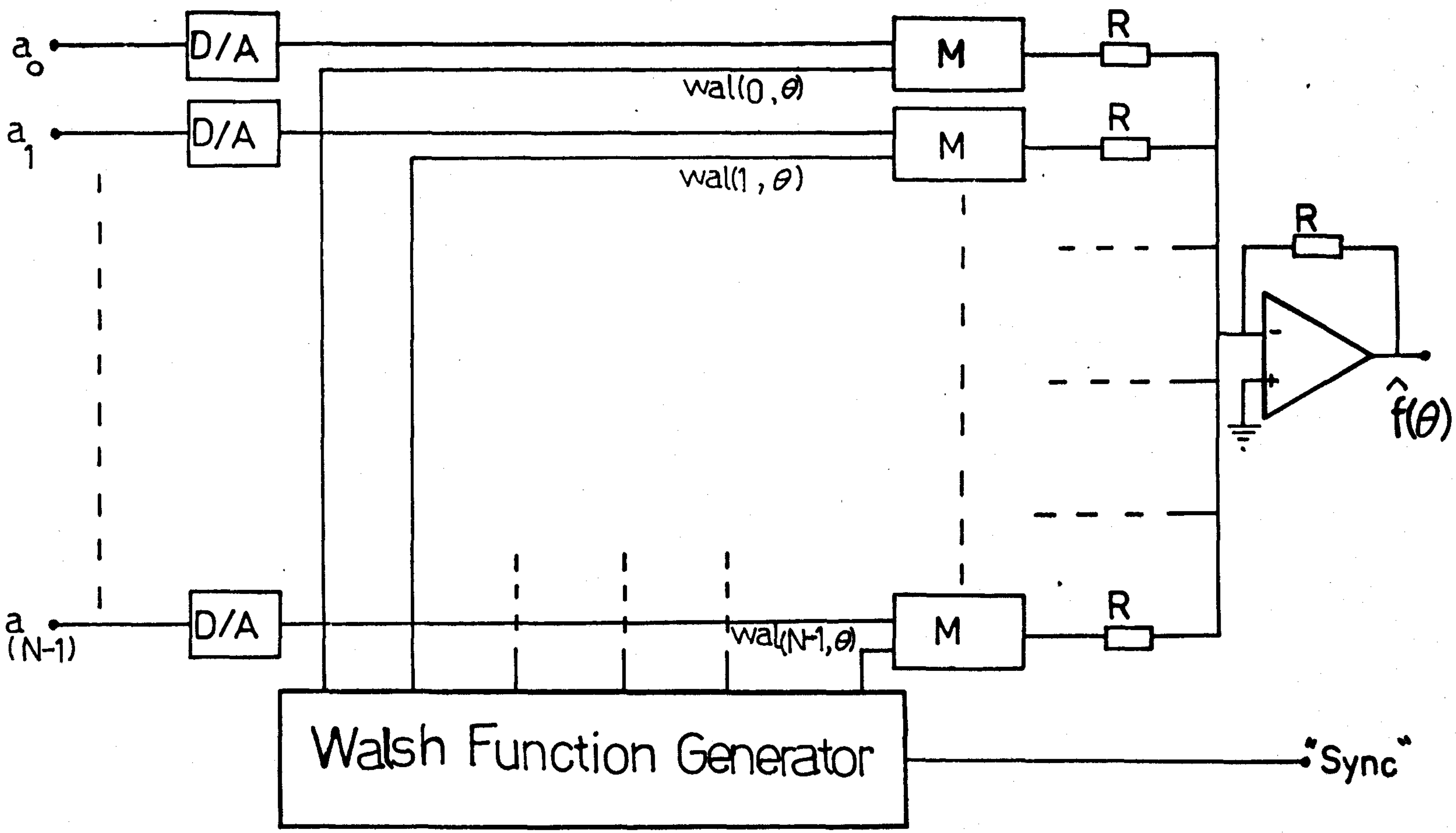

FIGURE 5: The Inverse Walsh Fourier Transform Circuit

3.1 THE WALSH FUNCTION GENERATOR:

The Walsh functions are binary in nature, and can be represented by pulses switching between the two voltage values corresponding to +1 and -1. The generation for the Walsh set can be implemented using digital circuits, representing the value +1 by a logical 1, and the value -1 by a logical 0.

The Walsh function can be generated in several ways. The simplest and straightforward one is to form the direct product of the correct Radmacher functions[3,8]. An n Radmacher function as defined by Equation (3) can be simply generated as the outputs from a synchronous n bit binary counter. The complete group of Walsh functions up to 2^n-1 sequence can be formed by using the multiplication property as given by Equation (5). Figure 6 shows the basic circuit for generating the set of Walsh functions as a product of Radmacher functions, (where 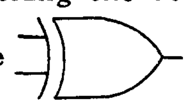 stands for the EXCLUSIVE OR operation). The main disadvantage of this circuit is that the generation of higher sequency terms depends on the generation of lower sequency terms. This yields different time delay for generating different sequencies, which increase rapidly as more bits are added to the binary counter, thereby limiting the speed of the generated Walsh set. Also, this timing error becomes critical when attempting to reproduce time varying functions from the Walsh domain, particularly at high frequencies which is the case in this work.

The Walsh function generator designed here has accurate timing of the zero crossings during the period θ for any generated Walsh sequences from 0 up to 64, and there are no "hazards" in the output. Any one

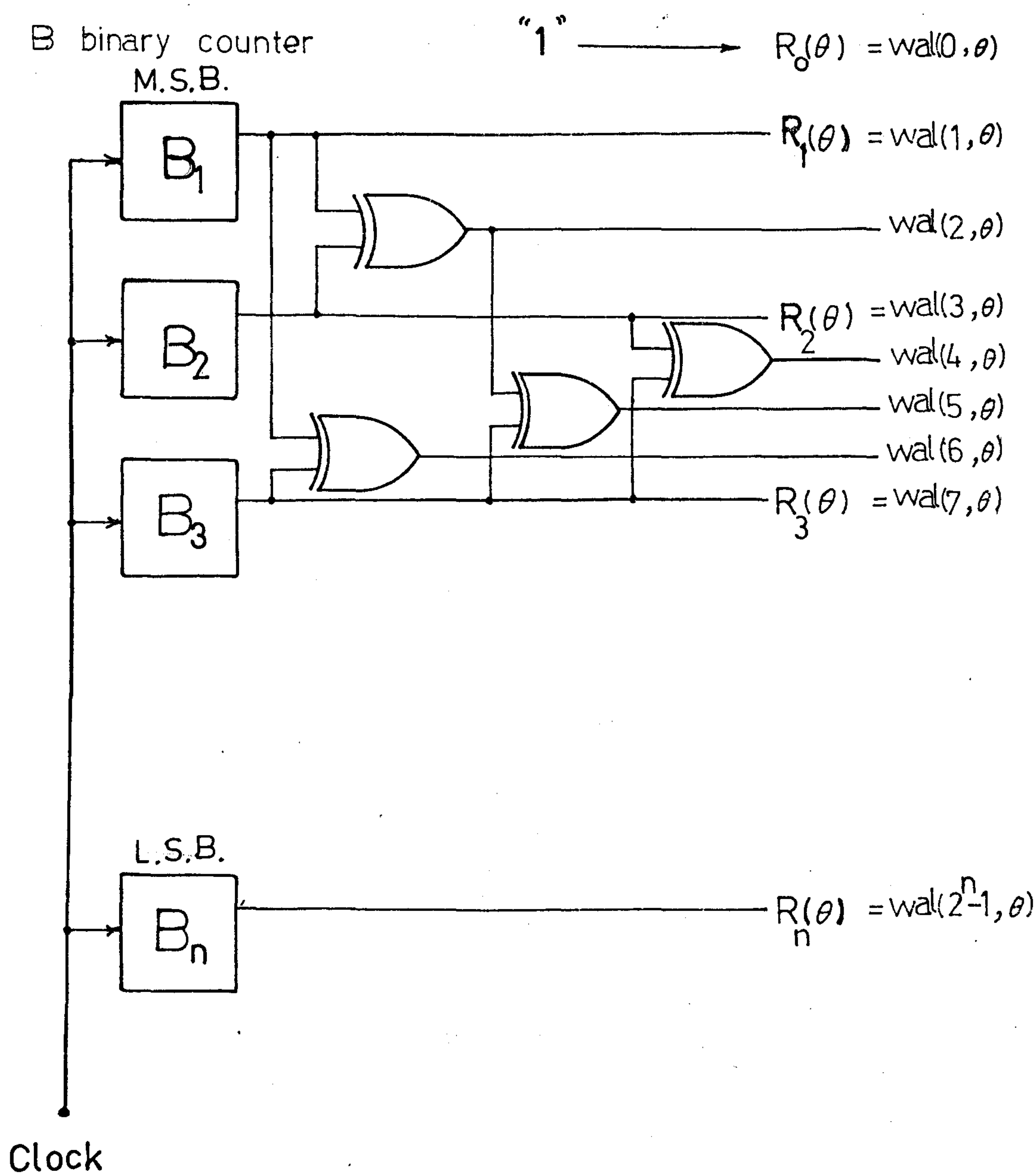

FIGURE 6: Walsh Function Generator as Product of Radmacher Functions

function can be generated according to the input of a standard binary code for the Walsh number. A "Sync" pulse is produced to determine the beginning of the time period θ.

A use of the rate multiplier[12,13] is made here to generate this Walsh set. The rate multiplier is so called because it gives a pulse train (or rate) that is the product of two inputs. It is an assembly of flip-flops and gates as shown in Figure 7. There are two inputs, the pulse frequency f which is the rate input, and a parallel number X in the range $0 \leq X < 1$. The output of the rate multiplier is a variable frequency pulse train equal to X times f.

Consider the binary counter in Figure 7 with n bits B_1, B_2, ..., B_n. The flip-flop used toggles at the falling edge of its input, and the clock rate of the counter has frequency f. Let the input to the AND gates G_1, G_2, ..., G_n be represented as: $f\overline{B}_1$, $fB_1\overline{B}_2$, ..., $fB_1B_2 \ldots B_{n-1}\overline{B}_n$, respectively. The output from the AND gates will be such that G_1 will have a pulse train of frequency f/2, G_2 a pulse train of frequency f/4, ..., and G_n having a pulse train of frequency $f/2^n$. No pulse of any of the trains ever coincides with a pulse of another train (this is the key for the operation of the rate multiplier). This allows ORing two or more of the pulse train together to obtain an output with a frequency that is the simple algebraic sum of the input frequencies. (This would be impossible if coincidence ever occurred.) Now by placing a number X, ($X = (X_1X_2 \ldots X_n)$ is its binary representation with X_1 the most significant bit having a weight of 2^{-1}, since $0 \leq X < 1$), on the gates $G_1G_2 \ldots G_n$ respectively, then the output of any gate G_i will occur or not occur according to whether the corresponding bit X_i is 0 or 1. Therefore the

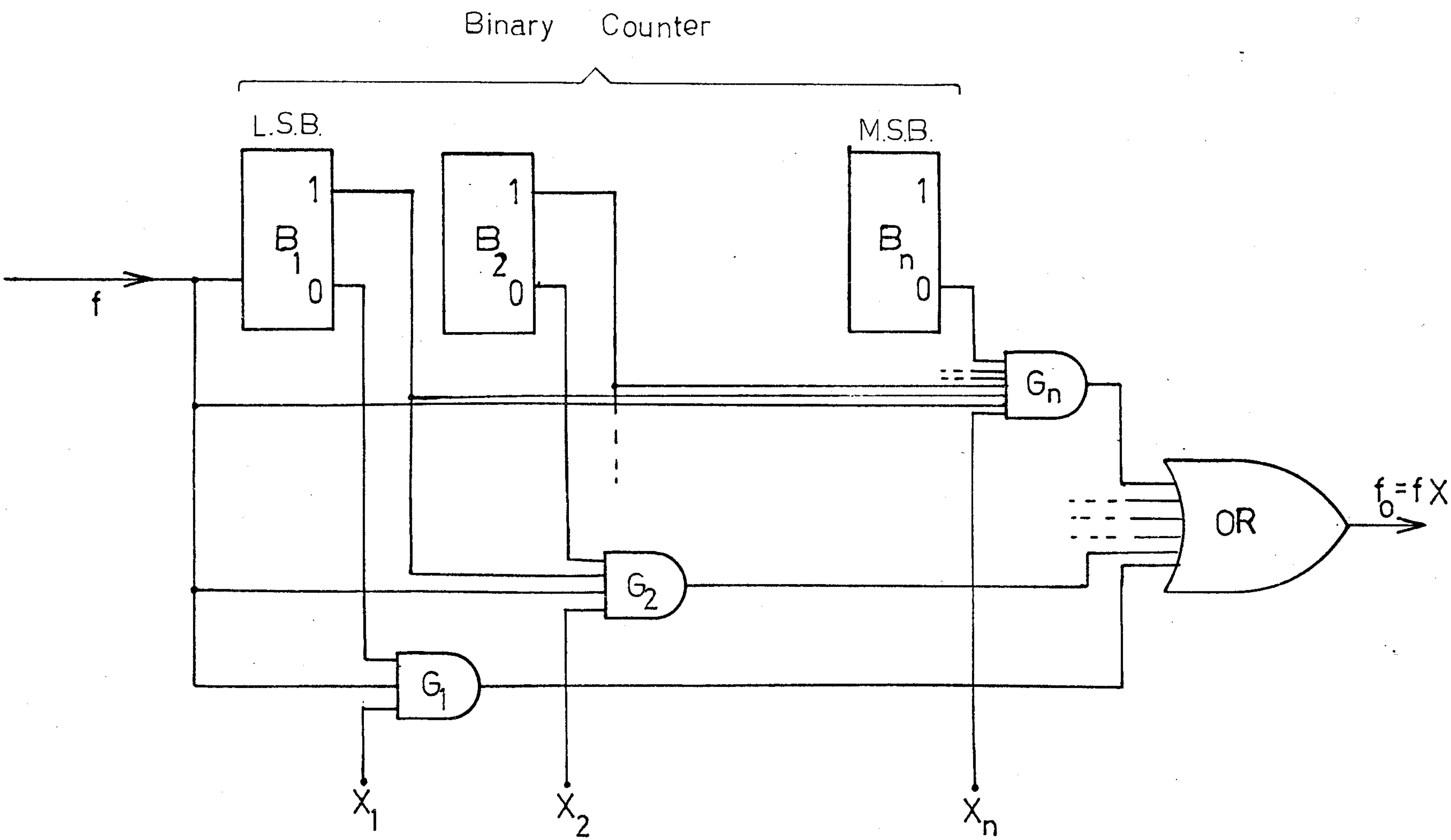

FIGURE 7: The Rate Multiplier

output frequency of the gate will be $X_i(f/2^i)$. Since the frequency out of the OR gate, f_o, will be the sum of the input frequencies, then

$$f_o = X_1(\frac{f}{2}) + X_2(\frac{f}{4}) + \ldots + X_n(\frac{f}{2^n})$$

$$= f(\frac{X_1}{2} + \frac{X_2}{4} + \ldots + \frac{X_n}{2^n})$$

$$= fX$$

The waveforms at each stage of the rate multiplier are shown in Figure 8 for n = 3. The number of binary stages is spoken of as the size of the rate multiplier. This determines the least fraction of the input frequency f one can get from the rate multiplier.

All the possible output pulse trains from the rate multiplier coincide with the zero crossings of the Walsh functions. If the output from an n bit rate multiplier is taken to toggle a flip-flop preset at the 1 state, then any Walsh function up to (2^n-1) can be generated for a given value of the X input. Figure 9 shows the rate multiplier output for n = 3 ordered such that each row differs by only one pulse from the preceeding row. The Walsh functions are shown too up to Wal(7,θ) as described before. The corresponding number X is listed which is found to be equal to the sequency of the Walsh function to be generated.

The schematic diagram for the designed Walsh function generator is shown in Figure 10. The size of the generator is 6 bits; this means that up to $2^6 = 64$ different sequency terms can be generated from it by setting a standard binary code for the sequency as shown. The generator

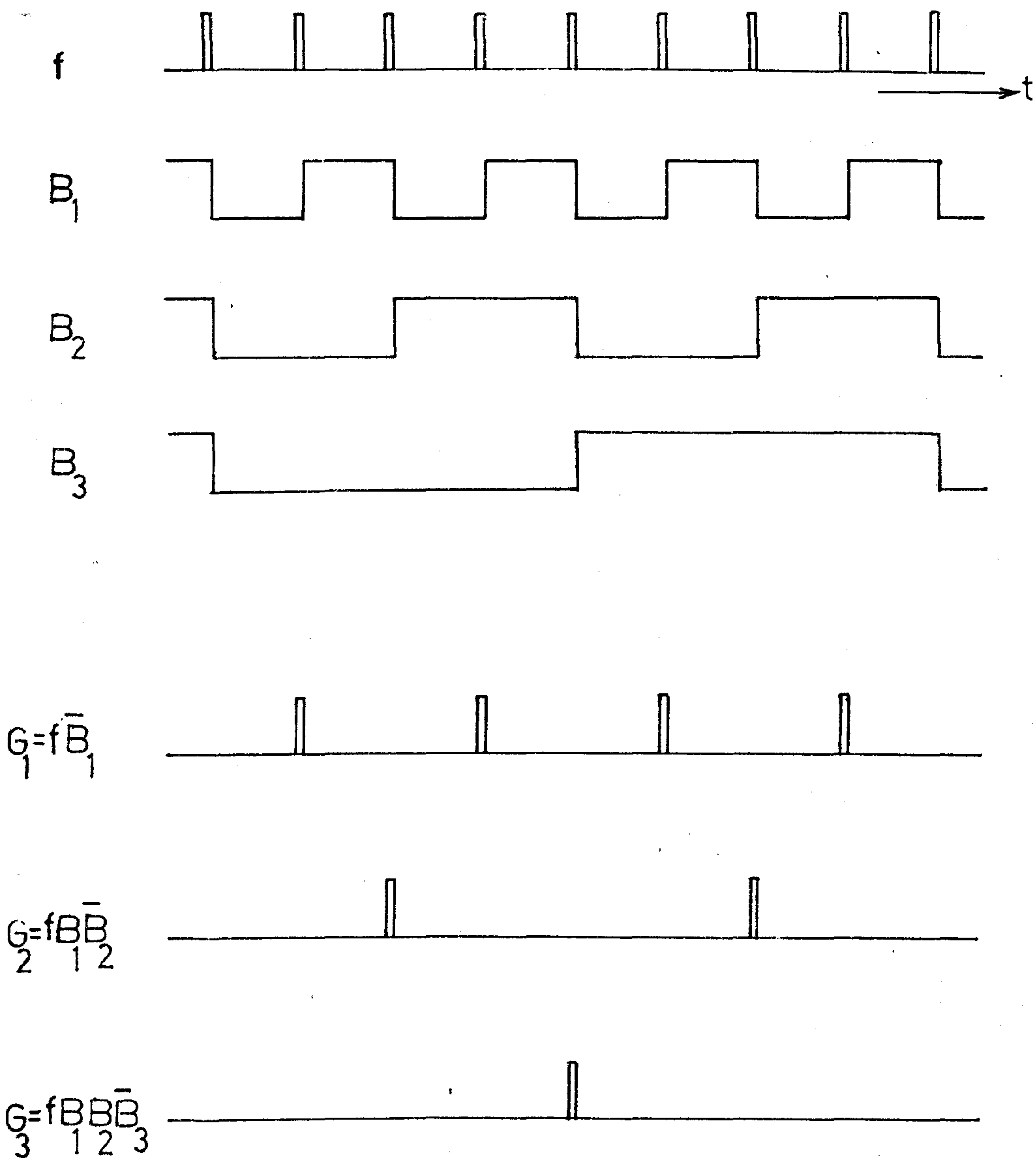

FIGURE 8: The Output States of the Rate Multiplier

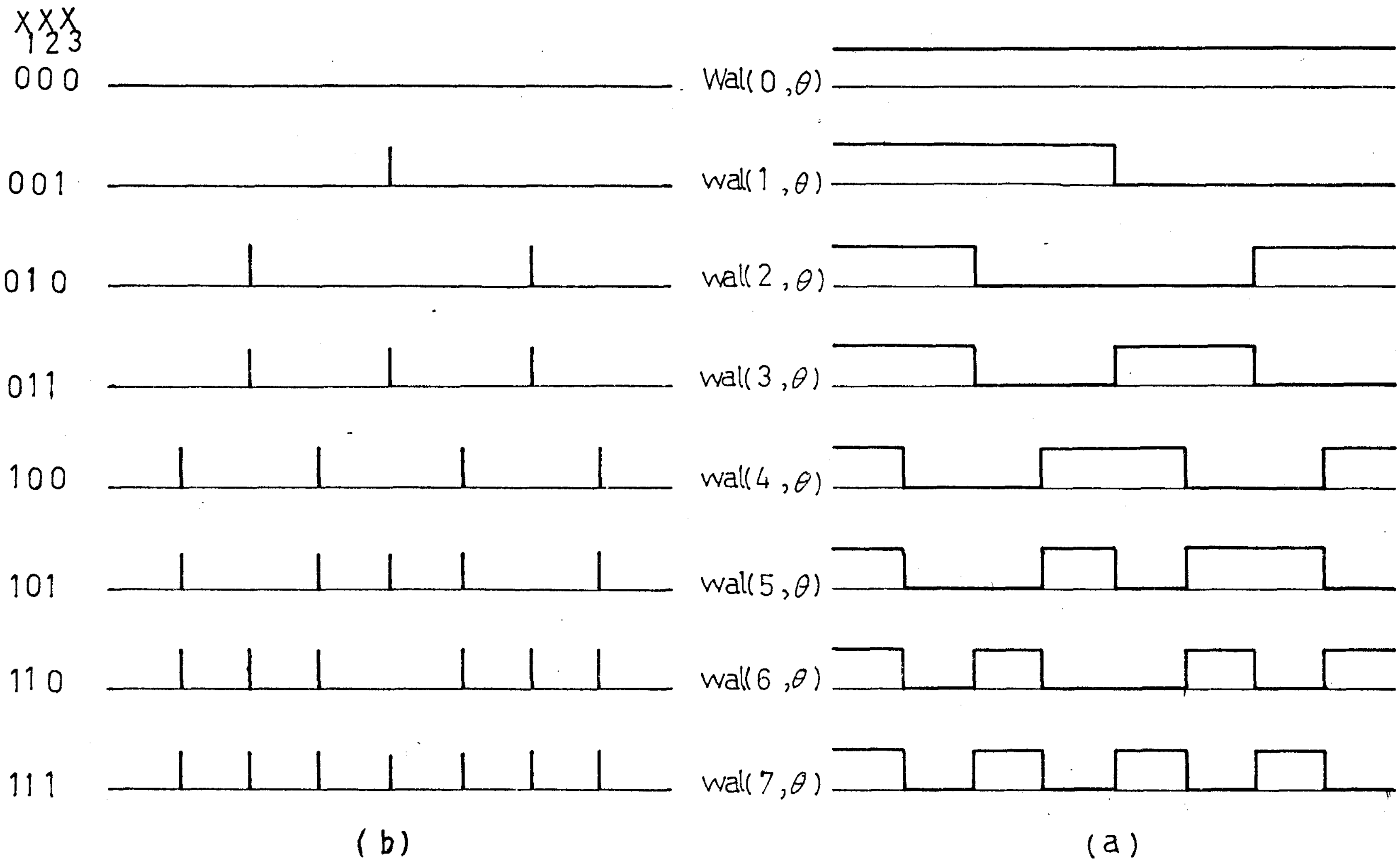

FIGURE 9: (a) The Outputs from a Flip-flop Toggled by the Possible Output of 3 Bit Rate Multiplier (b)

consists of a 6 bit synchronous up counter using J-K flip-flops, associated with the NAND and INVERTER logic gates using the standard 74H series modules. The circuit can work with a clock rate up to 10 MHz which is limited by the transition time required for the counter states to change. Higher speeds can be obtained by using a fully synchronous design. A manual preset to all 1's for the counter is necessary initially to ensure that the counter is in a correct starting state. A synchronizing pulse is produced to determine the beginning of the Walsh function generated, this pulse having a period equal to the time base of the Walsh function generated. The "Sync" pulse is used to preset the output flip-flop as shown. More Walsh functions could have been added by simply including one more flip-flop to the binary counter for every doubling of the number of functions required. However, this does cut down the speed of operation of the generator as designed.

The Walsh function generator described in Figure 10 can be divided into two stages, the first stage producing the pulse trains explained earlier (Figure 8). Let each train be called $\alpha_1, \alpha_2, \ldots, \alpha_n$. Then in the second stage, each pulse train α is fed to a separate AND gate with the associated Walsh data input. This process is shown in Figure 11. In this way more than one Walsh function can be generated at the same time using the same binary counter and gates G, since the output α's are the same for any Walsh function to be generated. The gates that deliver the α's can be chosen to be high current buffers to drive a large number of generators.

The output from the last gate G_6 in Figure 10, corresponding to α_6 in Figure 11 differentiates between the even and odd Walsh functions

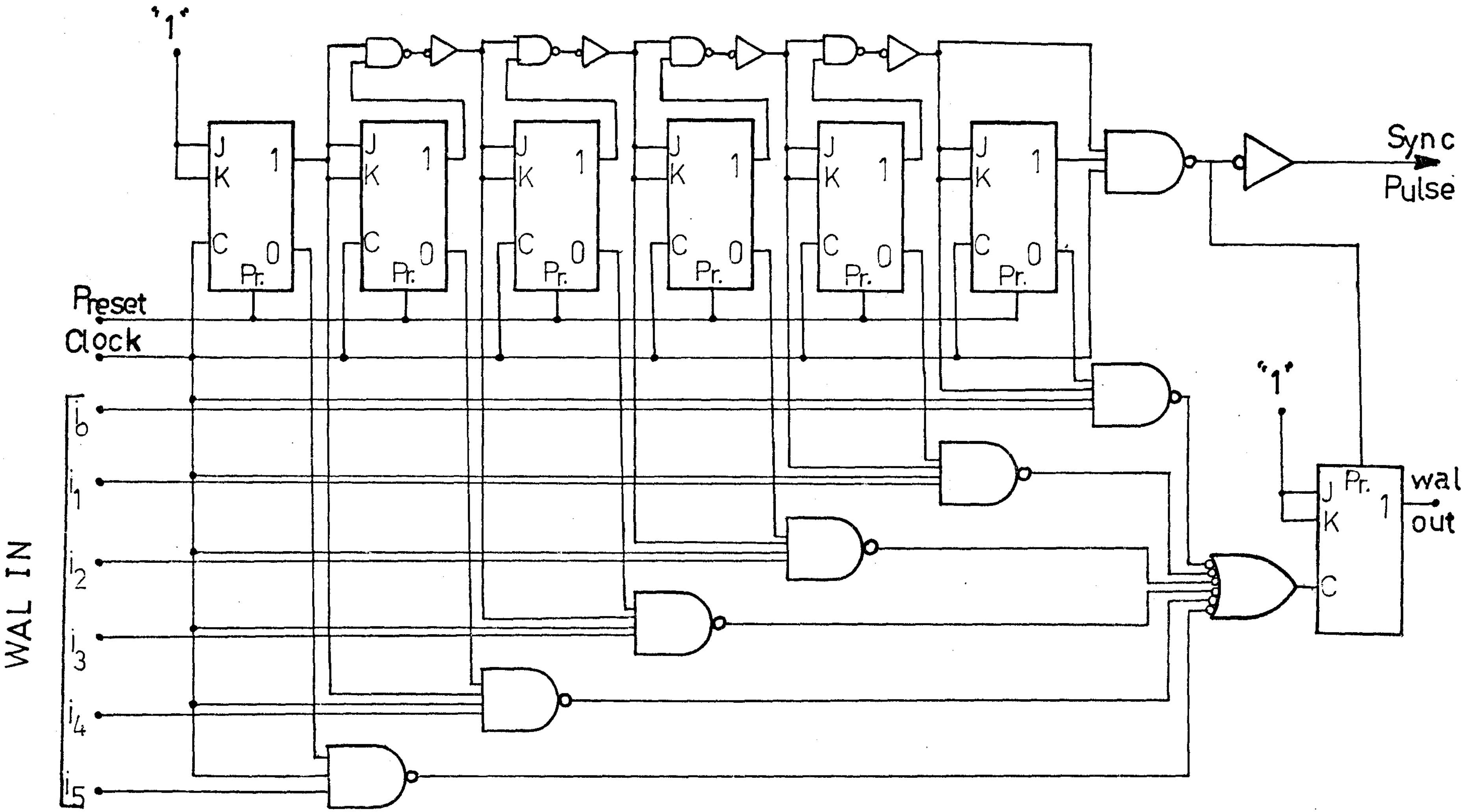

FIGURE 10: The Walsh Function Generator

FIGURE 11: Simultaneous Generation of Walsh Functions with the Same Counter

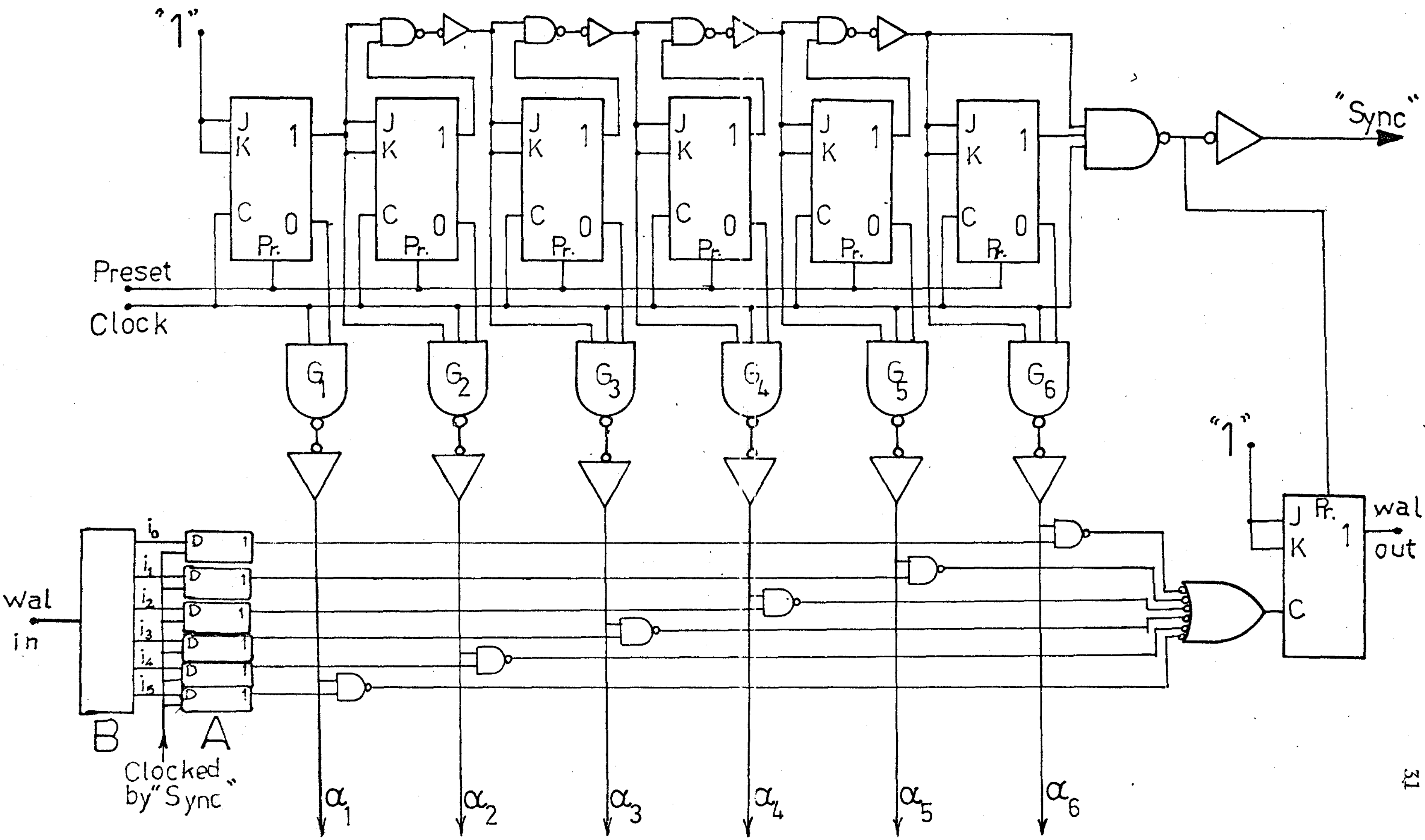

To be Used for Other Walsh Function Generators

Cal(i,θ) and Sal(i,θ). This is the pulse which makes the change in the function at the middle of its time base. Thus by eliminating this output from the OR gate we get only the even functions Cal(i,θ). By feeding this output constantly to the OR gate we produce always the odd functions Sal(i,θ). This process was used in the final design.

The sequency data input to the Walsh function generator must be able to change with every new period, since, in general, new information will be arriving each period. To do this, the sequency data is fed to the circuit through two D-type flip-flop registers as shown in Figure 11. The register A is clocked by the synchronizing pulse of the Walsh generator circuit and hence the input data is up-dated every period θ by accessing the data stored in register B. Register B can be loaded by a computer during the time interval θ, without disturbing the output of the generator.

The inverse Walsh transform instrument was designed to sum over 16 coefficients. Sixteen programmable Walsh function generators were built, 8 producing the even functions and 8 the odd functions. The final circuit used 2 basic binary counters clocked from the same master clock, each counter being used to generate 8 functions; four Cal(i,θ) and four Sal(i,θ). One "Sync" pulse was used to control the whole circuit. All 8 basic generators were mounted on one circuit board. The schematic diagram for the board containing the 8 Walsh function generators is shown in Figure 12. The input-output terminals are labelled with the appropriate number enclosed in a circle. They are identical for the two boards except for the "Sync" terminal which is taken as an output from one board and used as an input to the other. On Figure 12, the logic functions are

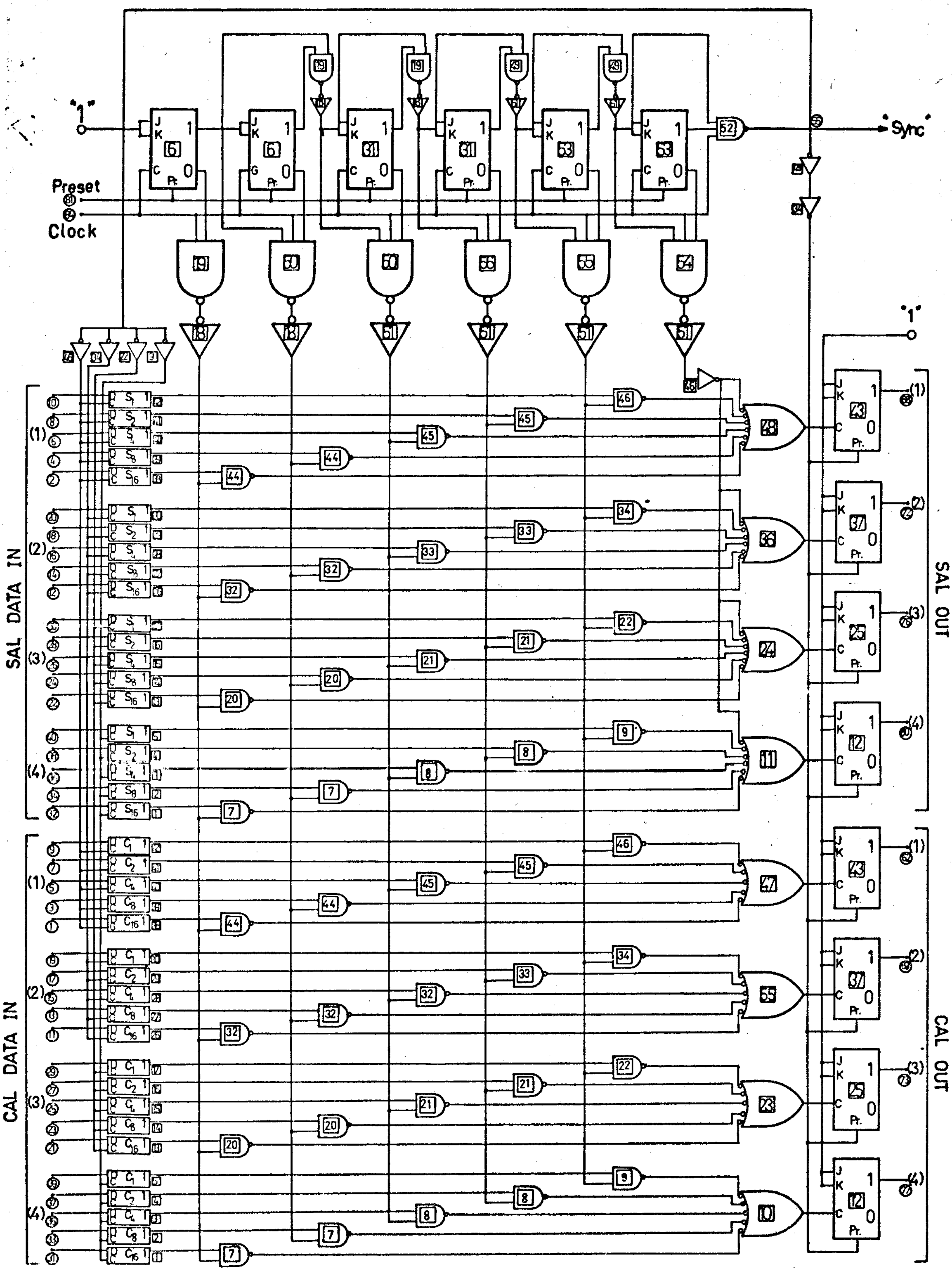

FIGURE 12: Schematic Diagram of Walsh Function Generator Card 1 or Card 2

labelled with numbers enclosed in squares. The same numbers appear in Figure B-1 (Appendix B) to show their location on the circuit board.

3.2 THE MULTIPLIER:

The second step in the inverse Walsh transformation is to multiply each coefficient input (a_i) with the corresponding Walsh function Wal(i,θ). This must be done for the 16 coefficients; therefore 16 multipliers were needed. This type of multiplication multiplies a voltage V_1 having arbitrary value with a voltage V_2 that can assume two values only. V_1 is the coefficient a_i which is constant during one period of the transform. V_2 is the Walsh function Wal(i,θ) switching between the two values +1 and -1. (In the generated Walsh function +1 was represented by a logical 1(+5V) and -1 by a logical 0(0V).)

Figure 13 shows an actual circuit used for analog multiplication by ±1, where V_1 may have any value within the voltage range of the operational amplifier. This circuit works as follows: If the FET is fully conducting, then the non inverting terminal (+) of the amplifier is grounded. V_0 must equal $-V_1$ to bring the inverting input terminal (-) also to ground potential. For FET non-conducting, the non-inverting terminal is at V_1 and the inverting terminal is also at V_1. This makes V_0 equal to V_1. This is a simple and ideal circuit for this type of multiplication, but with the operational amplifier available at a reasonable price it would only work with square waves up to 500 KHz.

The actual multiplier used in this design was a new integrated circuit (MC1496) designed to function originally as a modulator. The schematic diagram for the IC circuit is shown in Figure 14(a). In the final circuit (Figure 14(b)) the IC is connected as a modulator. The

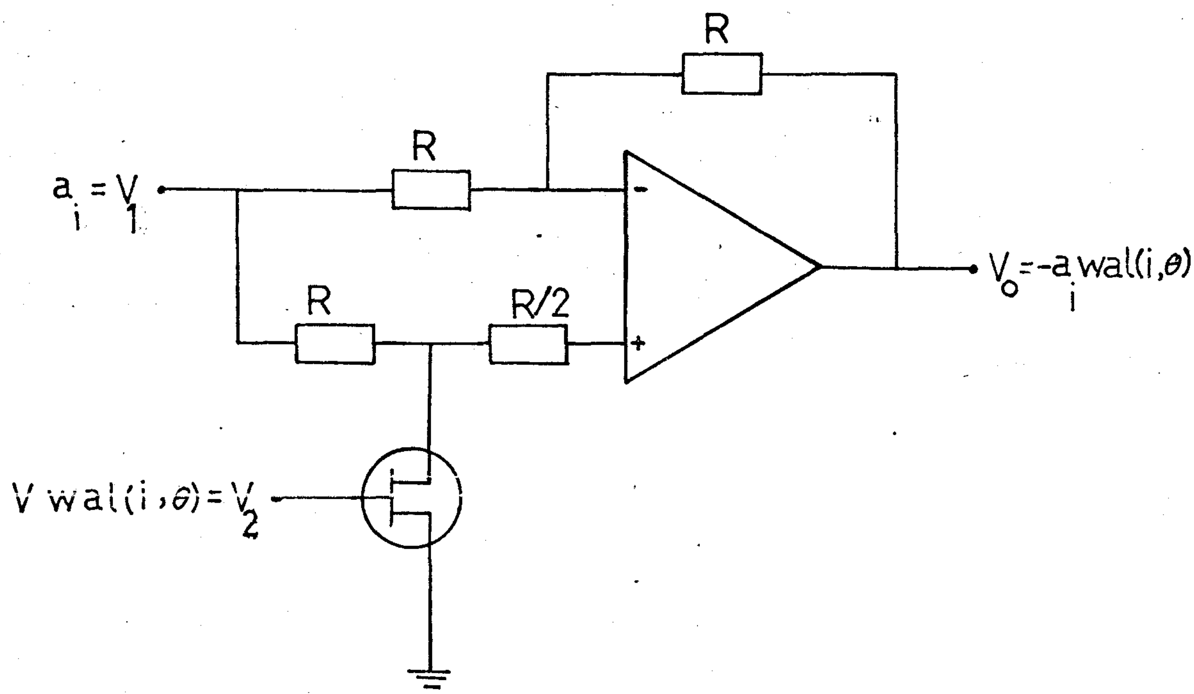

FIGURE 13: Analog Multiplication by ±1

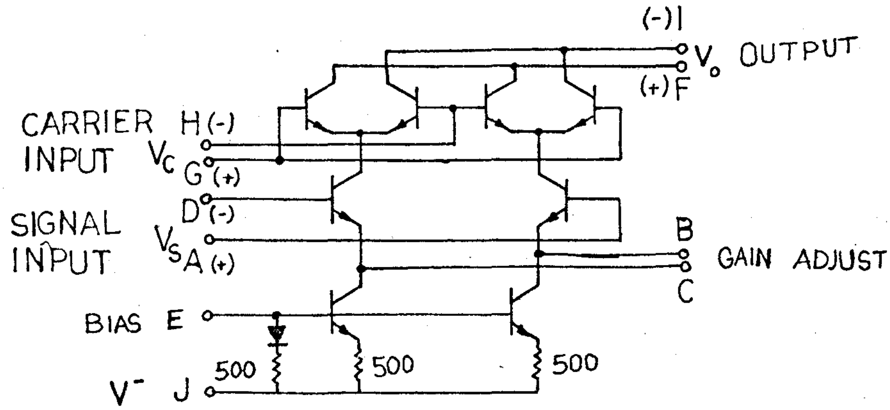

FIGURE 14(a): Schematic Diagram of MC1496

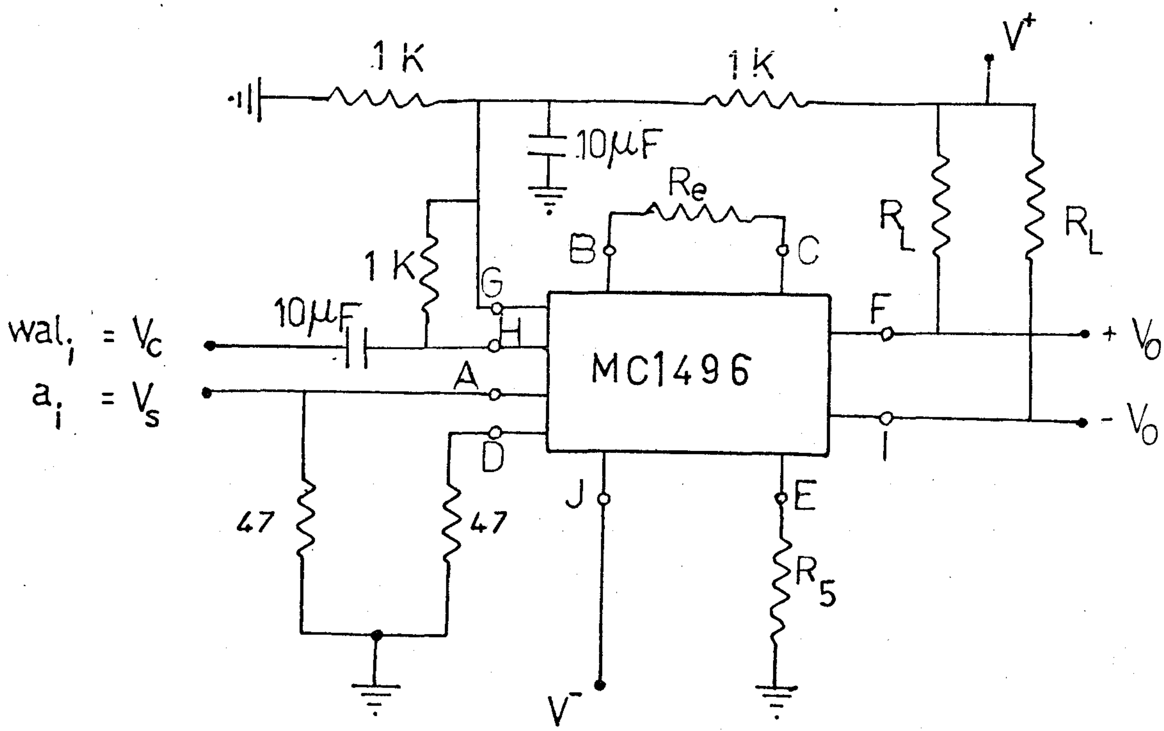

FIGURE 14(b): Multiplier Circuit

output will be the carrier signal (V_c) amplitude modulated with the signal (V_s). For linear operation, the input signal must be below a critical value determined by R_e and the bias current I_5 as:

$$V_s \leq I_5 R_e \tag{18}$$

where

$$R_5 = \frac{V^- - \phi}{I_5} \qquad \phi = 0.75V \text{ at } T_A = +25°C \tag{19}$$

The signal voltage gain is given by

$$A_{V_s} = \frac{V_o}{V_s} = \frac{R_L}{R_e + 2r_e} \qquad r_e = \frac{26mV}{I_5(mA)} \tag{20}$$

In the actual design, the coefficient a_i is placed at the V_s terminal as a d-c signal, while the Walsh function drives the carrier terminal V_C. The output for unity gain will give the Walsh function modulated with the coefficient magnitude. The output gain depends on the values R_L, R_e and R_5 as given by Equation (20). It was found that the best values for the resistances for almost unity gain were:

$$R_L = 820\Omega, \qquad R_e = 680\Omega, \qquad \text{and} \qquad R_5 = 4.7K\Omega.$$

The input coefficients had to be limited to ±1.2 volts for linear operation with accuracy of the circuit output less than 1%. This multiplier circuit worked up to 4 MHz. The d-c at the output terminal was suppressed by using a large capacitor of 10μF and 1 MΩ resistor.

The coefficient a_i was an analog voltage which was adjustable between the values ±1.2V. A high β transistor, resistor and potentiometer as shown in Figure 15 was built for each coefficient to produce a low output impedance voltage source for the coefficient. Two transistors in a Darlington configuration were required for better stability. Also, two potentiometers were used to give course and fine variations of a_i.

3.3 THE ADDER:

The adder was the final stage in the inverse Walsh transform design. This adder consists of a standard operational amplifier and resistors. The summation was made in two steps. The first one added four outputs from four multipliers together. Then the four outputs from the first adders were summed together to give the final output signal from the inverse transform circuit. The circuit diagram for the adder stage is shown in Figure 16. A high slew rate operational amplifier was used (NE531V). It was compensated with only one capacitor. The use of a 2N3819 FET in a feedback loop allowed the circuit to add 1 MHz square waves An amplification of about 3 could be made in the second stage adder by changing R and C to 15KΩ and 10pf, respectively.

All eight multipliers were mounted on one Vector board to work with the outputs from one board of the Walsh function generator. The associated two adders were mounted on the same board, one to sum over the four even terms and the other over the odd terms. One of the boards contained the final adder. The circuit diagram for each board is shown in Figure 17.

The connections for the multipliers as well as the adders are identical and hence only the connections for one multiplier and one adder are shown on the circuit diagram. The input output terminals are labelled with the appropriate number or letter enclosed in a circle. The IC's are

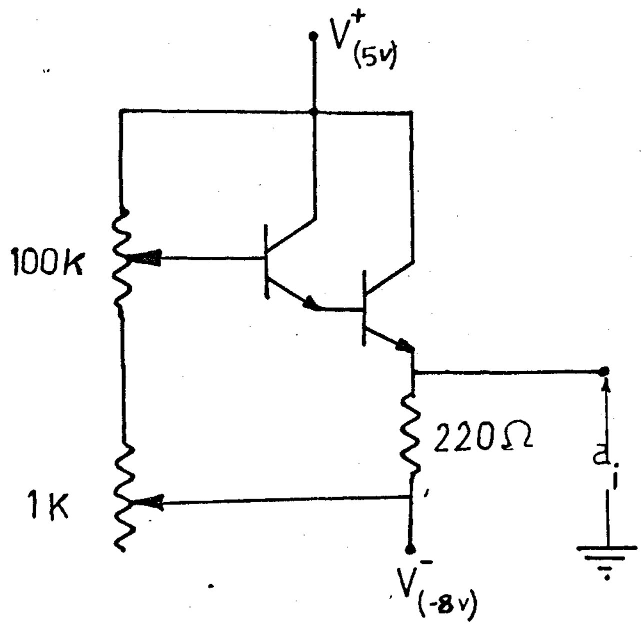

FIGURE 15: The Circuit for the Coefficient a_i

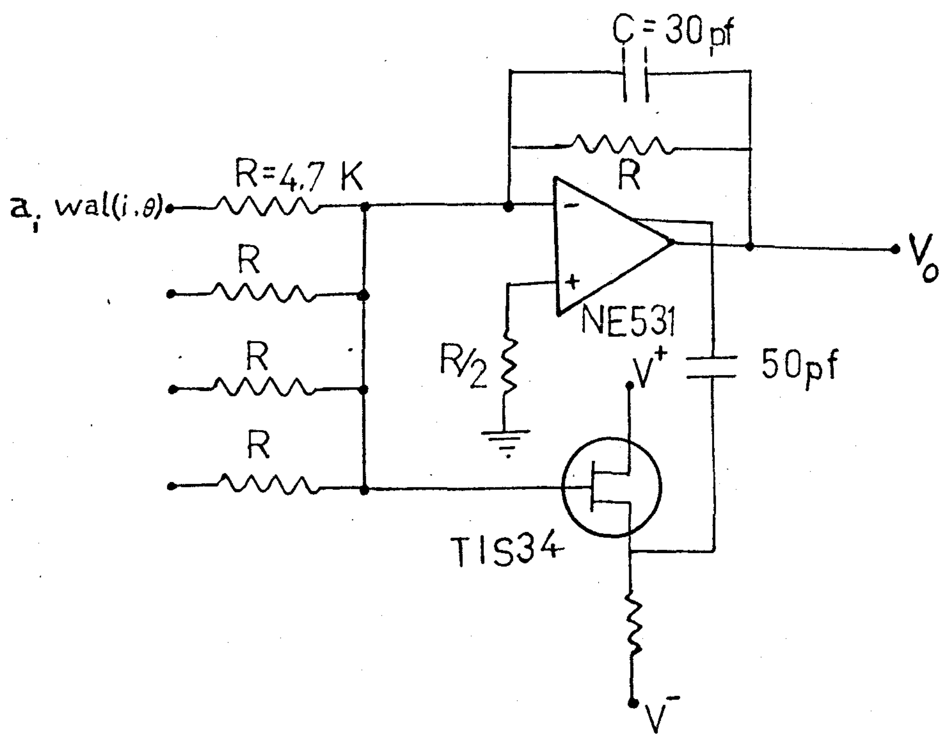

FIGURE 16: One Step Adder

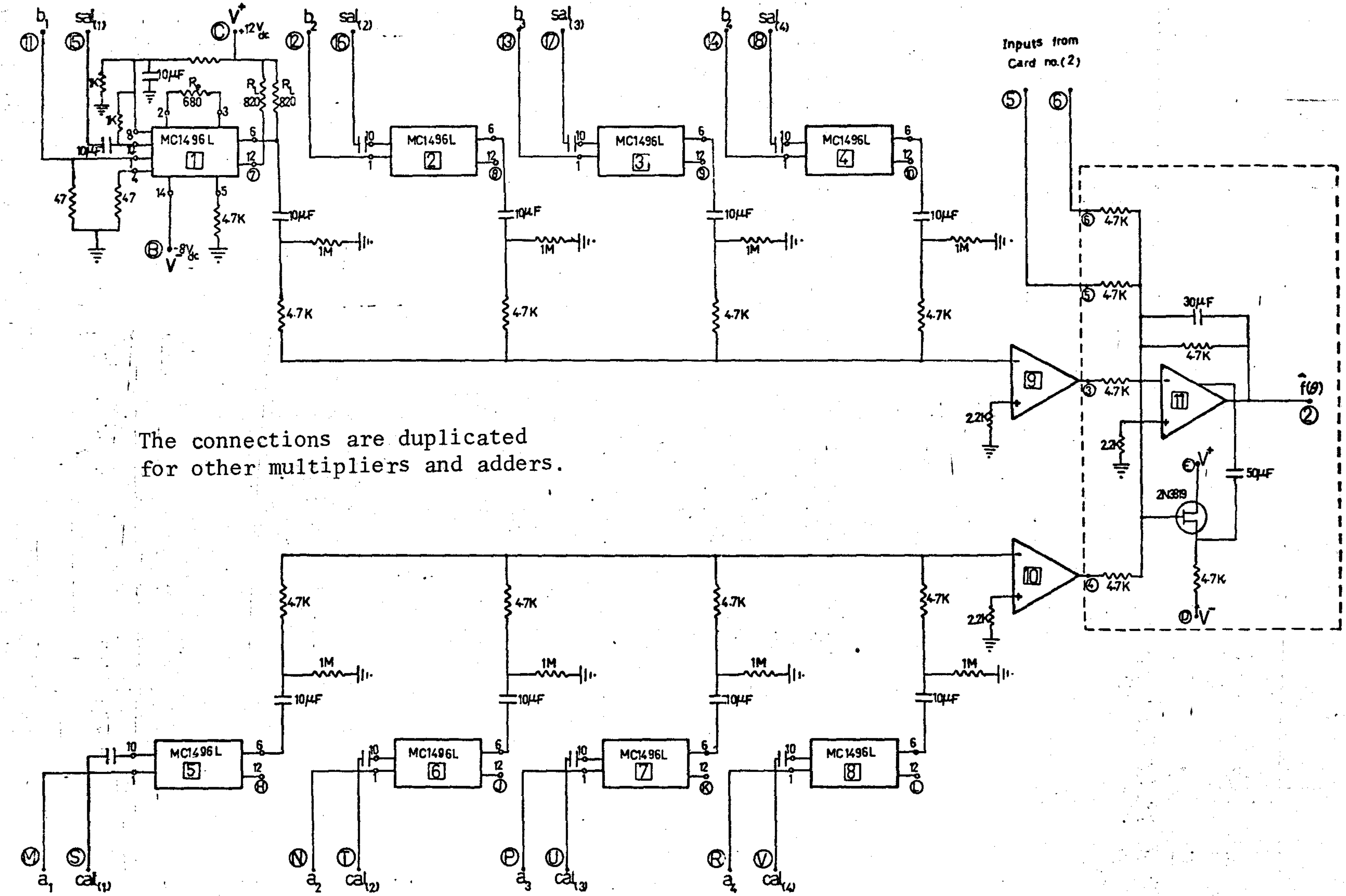

FIGURE 17: Schematic Diagram of the Multipliers and Summer Card 1 or Card 2. Dotted Part on Card 1 Only.

labelled with numbers enclosed in squares which are used to show their locations on the boards as in Figures B-2 and B-3 (Appendix B).

3.4 TESTING OF THE INSTRUMENT:

The inverse Walsh transform circuit has been tested for reconstruction of some known signals such as sinusoidal, ramp and triangle waveforms, using a limited number of the Walsh transform coefficients. The forward transform was obtained for these signals by computer simulation. The full set of transform coefficients are given in Appendix A. A selection of the dominant coefficients was made for the following three cases:

(i) Sinusoid: $f(\theta) = \sin\theta = \sum_{i=0}^{\infty} b_i \, Sal(i,\theta)$

The most dominant coefficients used for reconstruction of sin θ were:

$b_1 = 0.637$	$b_5 = -0.053$
$b_3 = -0.264$	$b_{31} = -0.031$
$b_7 = -0.127$	$b_{13} = -0.026$
$b_{15} = -0.063$	$b_{29} = -0.013$

(ii) Ramp: $f(\theta) = 3.2x\theta = \sum_{i=0}^{\infty} b_i \, Sal(i,\theta)$

The most dominant terms used for reconstruction of f(θ) were:

$b_1 = -0.8$	$b_8 = -0.1$
$b_2 = -0.4$	$b_{16} = -0.05$
$b_4 = -0.2$	$b_{32} = -0.025$

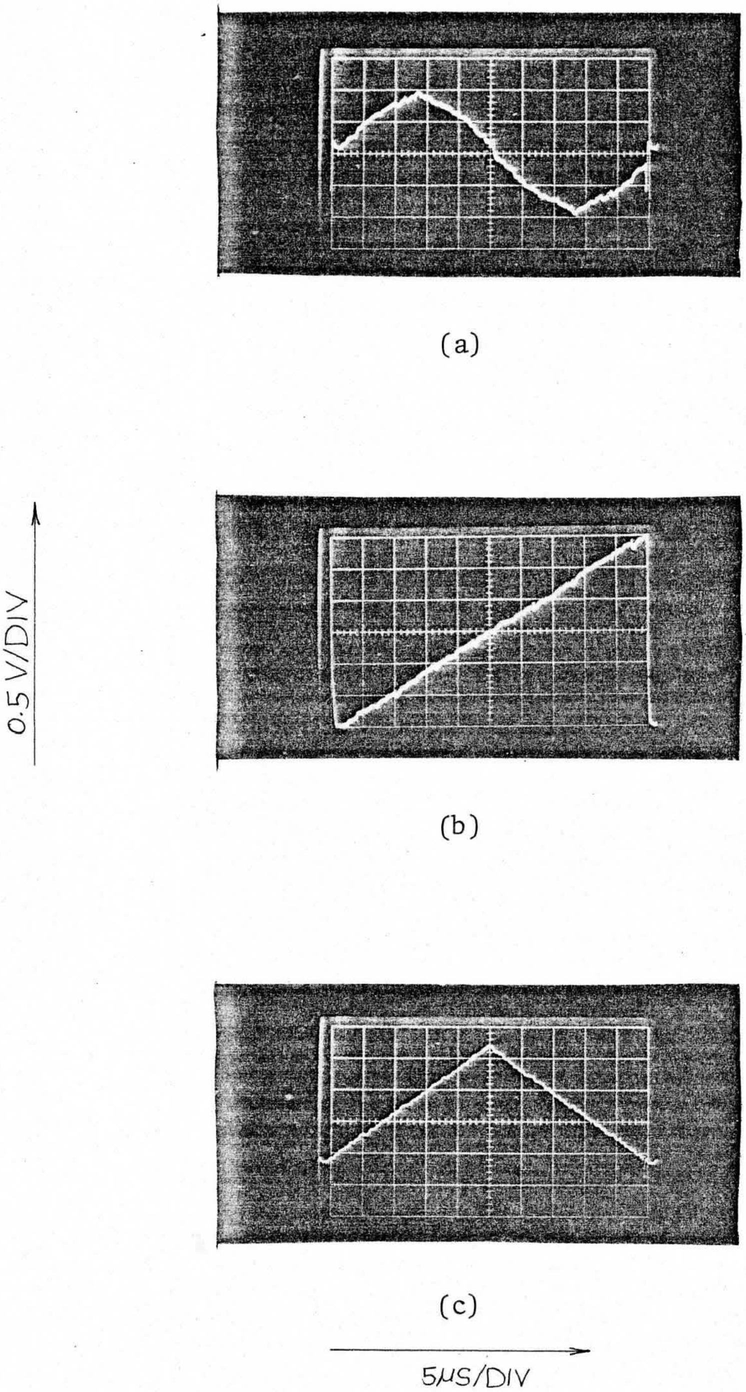

FIGURE 18: Reconstruction of Known Signals Using the Designed Instrument. (a) Sinusoid, (b) Ramp, and (c) Triangle.

(iii) Triangle: $f(\theta) = 4\theta \quad 0 \leqslant \theta < \frac{1}{2} = \sum_{i=0}^{\infty} a_i \, \mathrm{Cal}(i,\theta)$

$$= 4(1-\theta) \quad \frac{1}{2} \leqslant \theta < 1$$

The most dominant terms used for reconstruction of $f(\theta)$ were:

$a_i = -1$ $\qquad a_{15} = -0.125$

$a_3 = -0.5$ $\qquad a_{31} = -0.0625$

$a_7 = -0.25$

These results were entered into the apparatus for each case and the resulting waveforms are shown in Figure 18. These test waveforms verified the design of the apparatus in that dominant term synthesis of high frequency-periodic waveforms could be produced. The next chapter relates to the use of the apparatus for synthesizing video waveforms.

CHAPTER IV

INSTRUMENT APPLICATION ON A VIDEO SIGNAL

Due to the many inherent advantages of digital communication systems, research is being conducted by several investigators[1,5,10] in the field of image transmission in digital instead of analog form. Since images generally contain a large amount of information, the common problem in digital transmission is that high capacity channels are required to handle the data flow. Many studies have been made to reduce this capacity requirement. What makes this reduction possible is the examination and reduction of image redundancy, either statistically or psychovisually, since image points which are spatially close to each other tend to have nearly equal brightness levels.

Redundancy reduction can be made on an actual signal or any linear transformation. The redundancy of images appears in the Walsh domain such that the energy distribution will not be uniform, as in the spatial time domain, but rather only a few predominant coefficients contains most of the energy. Such distributions have been demonstrated for some scenes by H. C. Andrews and W. K. Pratt[1].

This chapter presents the results of using the inverse Walsh transform apparatus to reconstruct a video signal.

4.1 THE VIDEO SIGNAL:

A typical composite video signal for black and white television according to the United States standards, with reference to Television Engineering by Fink[14], is shown in Figure 19. The amplitude versus time graph gives a measure for the brightness of the picture elements with respect to time along a horizontal line of a picture from left to right. This is done by scanning an electron beam horizontally along this line of the picture. At the same time a vertical motion is given to the electron beam by a vertical sweep signal having a much slower velocity than the horizontal signal, but both are uniform. During the horizontal flyback time, the beam moves back to the left and then starts scanning a new line. This method is repeated to scan the whole picture, and this is done in 1/30 of a second. This method is known as "uniform linear scanning" which is universally used in television transmission. The highest frequency present in the video signal depends on the resolution of the picture elements, which determines the ability of producing the picture detail. In the American Standard Television System a 4.25 MHz bandwidth is reserved for transmitting the video information. This corresponds to 450 picture elements in the active time period of one line scan, and 525 lines are scanned per frame.

4.2 A WALSH TRANSFORM FOR THE VIDEO SIGNAL:

Consider the video signal f(t) in Figure 19. Since it is band limited to B Hz, say, then its maximum sequency is 2B zps as explained in Chapter II. A Walsh transform can be obtained for any period of the signal f(t), where this period will be the time base for the Walsh functions. Consider a period of f(t) as T such that $2BT = 2^n$, where n is an integer,

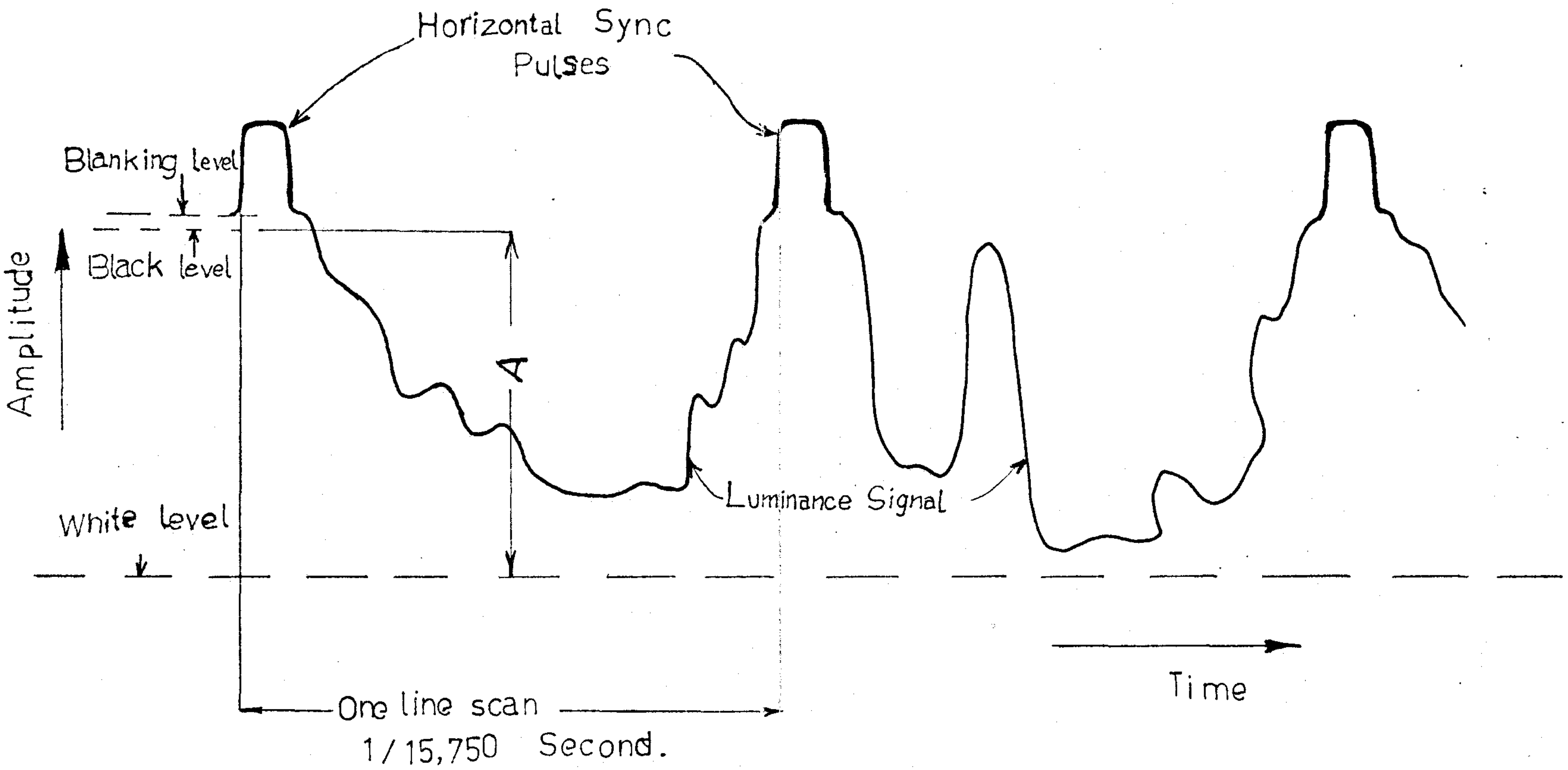

FIGURE 19: The Video Signal According to United States Standards

then the expansion of f(t) into a Walsh series is,

$$f(\theta) = \sum_{i=0}^{N-1} a_i \, Wal(i,\theta) \qquad \theta = 0,1,\ldots,N-1 \qquad (16)$$

where

$$a_i = \frac{1}{N} \sum_{\theta=0}^{N-1} f(\theta) \, Wal(i,\theta) \quad i = 0,1,\ldots,N-1 \qquad (17)$$

$$\theta = t/T, \; 0 \leqslant \theta < 1 \qquad\qquad N = 2^n = 2BT.$$

N in this case is exactly the number of picture elements to be scanned in the period T, which corresponds to the horizontal resolution of the image. The zero sequency term is a measure of the average brightness of the signal in the period T and is given by

$$a_o = \frac{1}{N} \sum_{\theta=0}^{N-1} f(\theta) \qquad (21)$$

The maximum value of a_o will not exceed the maximum value of the signal f(t). Let this maximum value equal A as shown in Figure 19 which is the difference between the white level and the black level. All the other Walsh coefficients will range between ±A/2.

The conservation of energy property exists between the time domain and the Walsh domain. The relation is such that

$$\frac{1}{N} \sum_{\theta=0}^{N-1} |f(\theta)|^2 = \sum_{i=0}^{N-1} a_i^2 \qquad (22)$$

This is analogous to Parseval's relationship for the Fourier analysis.

The errors produced due to Walsh domain quantization can be measured by the mean square error criteria. Let the quantized value of the coefficient a_i be referred to as a_{iq}; then the mean square error of the signal $f(\theta)$ from its representation in a normalized period $0 \leqslant \theta < 1$ is given by:

$$e^2 = \int_0^1 [f(\theta) - \sum_{i=0}^{N-1} a_{iq} \, Wal(i,\theta)]^2 d\theta$$

$$e^2 = \int_0^1 [\sum_{i=0}^{N-1} a_i \, Wal(i,\theta) - \sum_{i=0}^{N-1} a_{iq} \, Wal(i,\theta)]^2 d\theta$$

$$e^2 = \int_0^1 [\sum_{i=0}^{N-1} (a_i - a_{iq}) \, Wal(i,\theta)]^2 d\theta$$

$$e^2 = \sum_{i=0}^{N-1} (a_i - a_{iq})2 \qquad (23)$$

4.3 THE INSTRUMENT APPLICATION:

Figure 20(a) is an image scene and Figure 20(b) is the scanned signal along the horizontal line appearing on the scene. 256 sample points were taken in the period T shown (T $\approx$ the period of one line scan).

(a) A Picture Scene

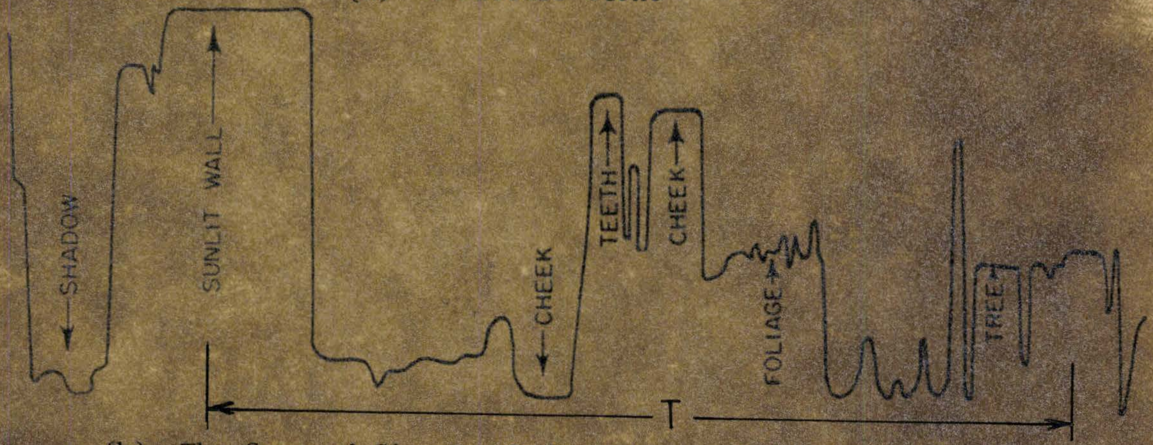

(b) The Scanned Signal of the Horizontal Line Appearing on the Scene. Taken from Television Engineering, by Fink, Chapter 1, pp. 10.

FIGURE 20: A Typical Video Signal

The period T was divided into four intervals and the Walsh transform obtained for each 64 successive samples being taken in each interval. The results are on pp. 63,64 in Appendix A.

A reconstruction for each of these four intervals was obtained using the inverse Walsh transform instrument. Only the 16 most dominant coefficients were used for signal reconstruction. The outputs were compared with the original signals as given in Figure 21.

A serious degradation is shown in the fourth interval. The 1^{st} and 4^{th} intervals were subdivided to two periods of 32 samples. A reconstruction of each period containing the 32 samples was made as shown in Figure 22. In the first half of the 1^{st} interval, 15 coefficients were used for signal reconstruction, but only two terms were needed to reconstruct the other half. 16 coefficients were used for each subinterval of the 4th interval which shows great improvement in the reconstructed signals.

4.4 THE TWO DIMENSIONAL WALSH FOURIER TRANSFORM:

The Walsh transform can be made on a two dimension sample of the image f(x,y). The chances for B.W. reduction may be greater in this case since each image point will tend to have the same brightness level as the surrounding points. However, the circuitry will be more complicated. The two dimensional Walsh transform is given as:

$$f(x,y) = \sum_{i=0}^{N-1} \sum_{j=0}^{M-1} a_{ij} \, \mathrm{Wal}(i,x) \, \mathrm{Wal}(j,y) \qquad (24)$$

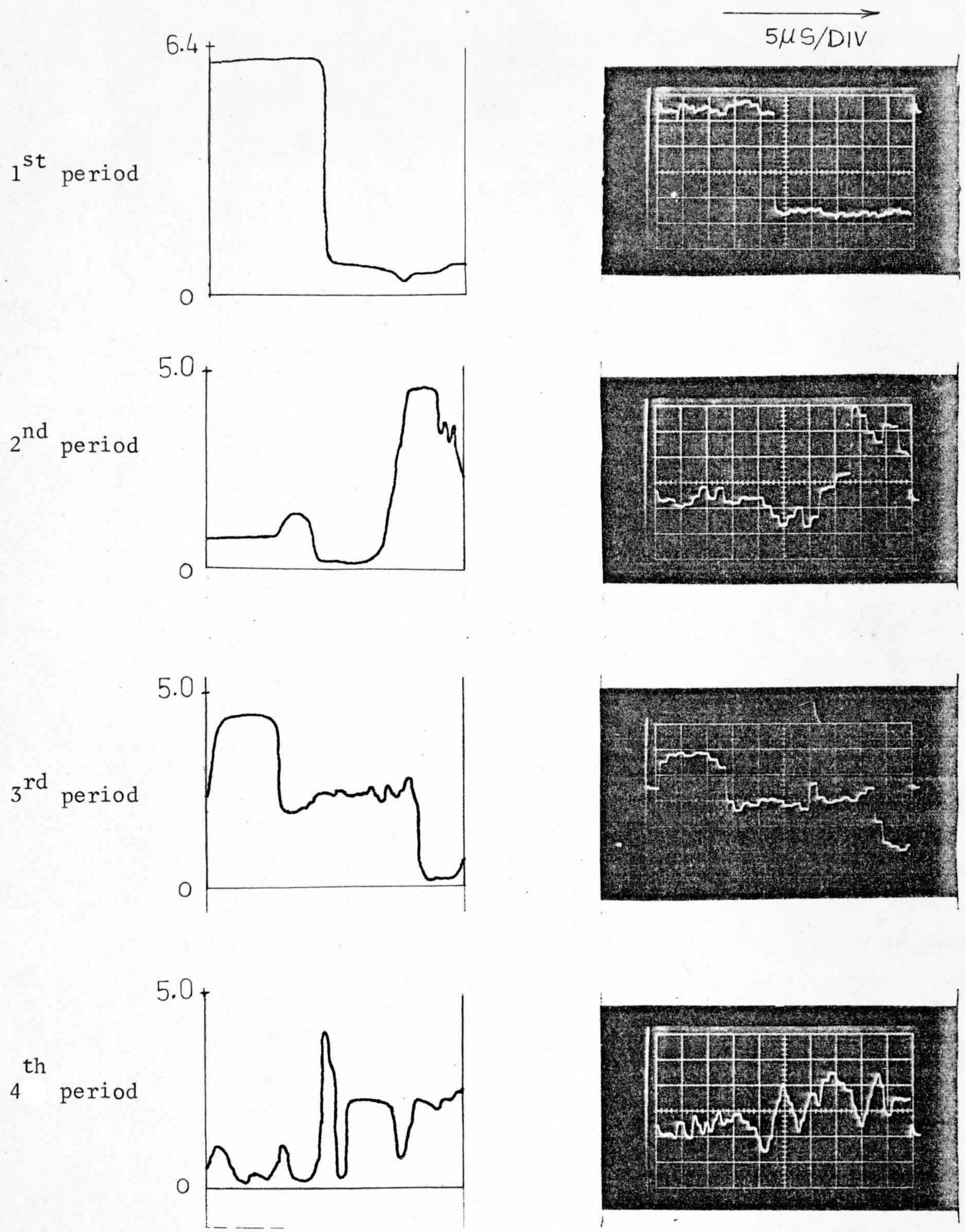

Original Signal

Reconstructed Signal Using the 16 Dominant Terms

FIGURE 21: Reconstruction for the Four Intervals of the Video Signal. Each Interval Contains 64 Samples

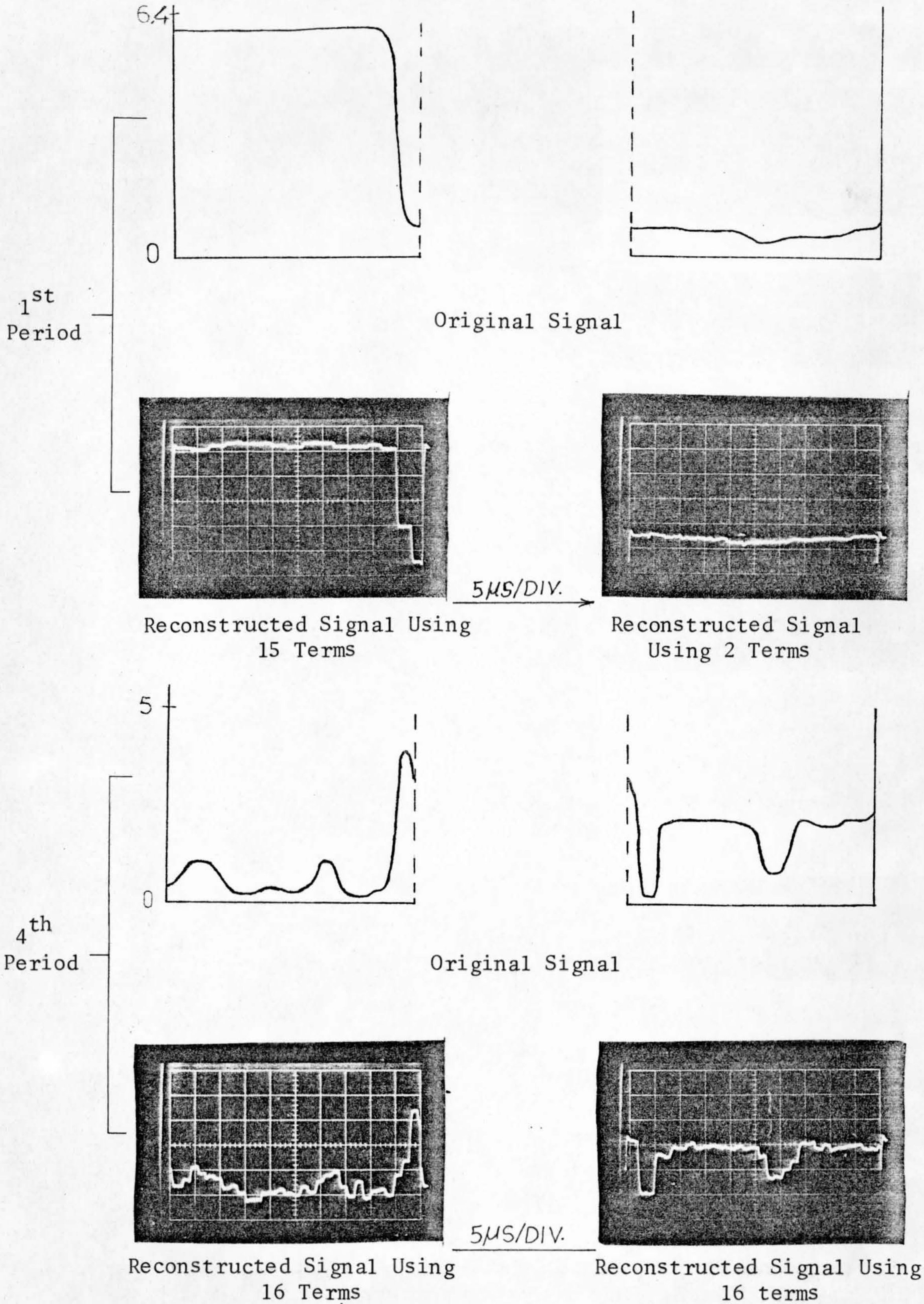

FIGURE 22: Reconstruction for an Interval of 32 Samples of the Video Signal

and the coefficients can be determined from:

$$a_{ij} = \frac{1}{NM} \sum_{x=0}^{N-1} \sum_{y=0}^{M-1} f(x,y)\, \text{Wal}(i,x)\, \text{Wal}(j,y) \qquad (25)$$

N and M represents the resolution in the two dimension x, y. A scanner transforms this two dimensional array into a one dimensional sequence ready for transmission over the channel.

CHAPTER V

CIRCUIT DESIGN ERRORS AND LIMITATIONS

The errors produced in the inverse Walsh transform instrument are mainly due to two aspects. The first one is the mathematical approximation involved in the design, by using a finite number of terms of the transform to reconstruct the original signal. The second one is due to errors produced in the built circuit. Both types of error are discussed throughout this chapter.

5.1 MATHEMATICAL ERROR:

There are N Walsh Fourier coefficients for N samples representing any band limited signal $f(\theta)$ in the normalized period $0 \leq \theta < 1$. The Walsh transform for the signal $f(\theta)$ and its inverse are given by Equations (16) and (17).

In the designed instrument the inverse Walsh transform is performed over a limited number of coefficients which is 16 terms, out of the total number N that can reach up to 64. Theoretically, an exact reconstruction of the signal $f(\theta)$ can be obtained for $N = 16$ (except for circuitry error). There are three choices for N in this design, 16, 32 or 64. (Note that the design is flexible to period variations according to the Walsh function property given by Equation (7).)

Measuring this error by the mean square error criteria, then the mathematical design error over the period $0 \leq \theta < 1$ referred to Equation (23) will be given by:

$$e^2 = \sum_{\text{over}(N-16)\text{ terms}} a_i^2 \qquad (26)$$

where 16 represents the 16 terms out of the total number N, used for signal reconstruction.

5.2 CIRCUITRY ERROR:

There are three stages in the designed instrument; the Walsh function generator, the multipliers and the summer. In the Walsh function generator stage there are no errors since the generator has accurate timing for any sequency term to be generated. The circuit error produced only in the multiplier and summer will be discussed.

(a) Multiplier Error: The input coefficients to the multipliers are limited for linear operation to an absolute value of ≈ 1.2V, with an error of less than 0.01V. This error actually allows for up to 128 quantization levels to be used for the Walsh transform coefficient.

Another error is produced in the multiplier due to the main function of the circuit. The MC 1496 function originally as a modulator, the carrier suppression is achieved by changing the d-c level at the signal terminal. Since we placed the d-c coefficient value at the signal terminal to modulate the Walsh function feeding the carrier terminal, therefore the reading at the signal input for zero carrier output must be taken into account when feeding the coefficients to the inverse Walsh instrument by subtracting it from the input coefficient.

(b) Adder Error: The errors produced in the multiplier are partially added in the final stage. This error increases as the number of terms included in the inverse transform increase. For the total of 16 coefficients, the output reading for zero inputs is about 0.05V. This error limits the number of quantization levels of the transform to 32. Using only 8 terms of the Walsh coefficients, the number of quantization levels can be increased to 64.

The effect of circuitry error is actually in limiting the number of quantization levels used for the transform. The errors would be the same as that due to quantization as given by Equation (23). A comparison must be made between the number of quantization levels and the number of terms included in the Walsh transform, since increasing the number of quantization levels for better signal reproduction will increase the number of terms in the inverse transform which leads to greater error. It is obvious that the number of terms included in the inverse transform will be smaller for smaller periods of the transform.

CHAPTER VI

CONCLUSIONS

The instrument designed in this work for the inverse Walsh transform restricts the absolute amplitude of the coefficients to $\approx$ 1.2V. This allows up to 64 quantization levels for the transform if the sum is made over 8 terms and 32 quantization levels for 16 terms included in the inverse transform. The maximum sequency term the apparatus can reach is up to 64 in one period. The instrument will only reconstruct a 1 MHz square wave, being limited by the adder in the final stage. A reconstruction of some known signals such as sinusoid, ramp and triangle were obtained by using as few as five coefficients which gave a very good reconstructed signal.

Analysis of a video signal was made and the results were used in the inverse Walsh transform instrument to reconstruct the signal by using a limited number of the Walsh coefficients. The results were shown, but the effect of approximation can be made only by observing the whole picture. The errors are discussed following the mean square error criteria which is mathematically tractable. However, for images, the quality is defined in subjective terms and can only be measured in terms of observer response which is very difficult to measure. Future study on this subject should probably be in the area of statistical research for the effect of Walsh transform coding on the reproduced image scenes.

APPENDICES

APPENDIX A

The Walsh Transform for Specific Signals

A-1 The Walsh Transform of a Sinudoidal Signal

Walsh no.					
0 → 4	-.0000	.6366	.0000	-.0000	-.0000
5 → 9	-.2637	.0000	-.0000	-.0000	-.0525
10 → 14	-.0000	.0000	-.0000	-.1266	.0000
15 → 19	-.0000	.0000	-.0125	-.0000	.0000
20 → 24	.0000	.0052	-.0000	.0000	.0000
25 → 29	-.0260	-.0000	.0000	.0000	-.0627
30 → 34	.0000	-.0000	.0000	-.0031	.0000
35 → 39	-.0000	.0000	.0013	-.0000	.0000
40 → 44	.0000	.0003	-.0000	.0000	.0000
45 → 49	.0006	.0000	-.0000	.0000	-.0062
50 → 54	-.0000	-.0000	-.0000	.0026	.0000
55 → 59	.0000	-.0000	-.0130	0.0000	.0000
60 → 63	-.0000	-.0313	0.0000	-.0000	

A-2 The Walsh Transform of a Ramp Signal

Walsh no.					
0 → 4	.50000	-.25000	0.00000	-.12500	0.00000
5 → 9	0.00000	0.00000	-.06250	0.00000	0.00000
10 → 14	0.00000	0.00000	0.00000	0.00000	0.00000
15 → 19	-.03125	0.00000	0.00000	0.00000	0.00000
20 → 24	0.00000	0.00000	0.00000	0.00000	0.00000
25 → 29	0.00000	0.00000	0.00000	0.00000	0.00000
30 → 34	0.00000	-.01563	0.00000	0.00000	0.00000
35 → 39	0.00000	0.00000	0.00000	0.00000	0.00000
40 → 44	0.00000	0.00000	0.00000	0.00000	0.00000
45 → 49	0.00000	0.00000	0.00000	0.00000	0.00000
50 → 54	0.00000	0.00000	0.00000	0.00000	0.00000
55 → 59	0.00000	0.00000	0.00000	0.00000	0.00000
60 → 63	0.00000	0.00000	0.00000	-.00781	

A-3 The Walsh Transform of a Triangle

Walsh no.					
0 → 4	.50000	0.00000	-.25000	0.00000	0.00000
5 → 9	0.00000	-.12500	0.00000	0.00000	0.00000
10 → 14	0.00000	0.00000	0.00000	0.00000	-.06250
15 → 19	0.00000	0.00000	0.00000	0.00000	0.00000
20 → 24	0.00000	0.00000	0.00000	0.00000	0.00000
25 → 29	0.00000	0.00000	0.00000	0.00000	0.00000
30 → 34	-.03125	0.00000	0.00000	0.00000	0.00000
35 → 39	0.00000	0.00000	0.00000	0.00000	0.00000
40 → 44	0.00000	0.00000	0.00000	0.00000	0.00000
45 → 49	0.00000	0.00000	0.00000	0.00000	0.00000
50 → 54	0.00000	0.00000	0.00000	0.00000	0.00000
55 → 59	0.00000	0.00000	0.00000	0.00000	0.00000
60 → 63	0.00000	0.00000	-.01563	0.00000	

A-4 A Typical Video Signal

(Fig. 20-b, 256 samples in the period T)

Sample no.								
0 → 7	6.0	6.0	6.0	6.0	6.0	6.0	6.0	6.0
8 → 15	6.0	6.0	6.0	6.0	6.0	6.0	6.0	6.0
16 → 23	6.0	6.0	6.0	6.0	6.0	6.0	6.0	6.0
24 → 31	6.0	6.0	5.9	5.8	3.5	1.2	.8	.8
	.8	.8	.8	.8	.8	.8	.7	.7
	.7	.7	.7	.7	.7	.6	.6	.4
	.4	.4	.5	.6	.6	.6	.6	.6
56 → 63	.6	.6	.6	.7	.8	.8	.8	.8
	.8	.8	.8	.8	.8	.8	.8	.8
	.8	.8	.8	.8	.8	.8	.8	.8
	.8	1.2	1.3	1.4	1.4	1.4	1.4	1.3
	1.2	.6	.3	.2	.2	.2	.2	.2
	.2	.2	.2	.2	.2	.2	.2	.2
	.2	.2	.4	.8	1.2	1.6	2.8	3.2
	3.6	4.6	4.6	4.6	4.6	4.6	4.6	4.6
120 → 127	4.6	3.4	3.8	3.2	3.6	3.6	3.0	2.4
	2.4	3.4	4.0	4.2	4.4	4.4	4.4	4.4
	4.4	4.4	4.4	4.4	4.4	4.4	4.4	4.4
	4.4	4.2	2.0	2.0	2.0	2.0	2.0	2.1
	2.2	2.2	2.3	2.4	2.4	2.4	2.4	2.3
	2.5	2.5	2.4	2.3	2.3	2.4	2.4	2.4
	2.4	2.6	2.4	2.2	2.2	2.6	2.4	2.3
	2.3	2.3	2.4	2.7	2.8	2.2	2.0	.4
	.3	.3	.2	.2	.2	.3	.3	.4
	.5	.8	1.0	1.1	1.0	.9	.6	.3
	.2	.2	.2	.4	.4	.4	.3	.2
	.3	.4	.6	1.1	1.1	.4	.3	.2
	.2	.2	.3	.4	.6	2.4	4.0	3.2
	2.8	.3	.2	1.8	2.2	2.2	2.2	2.2
	2.2	2.2	2.2	2.2	2.2	2.2	2.1	2.0
	1.8	.8	.8	1.0	1.4	2.2	2.2	2.1
248 → 255	2.1	2.0	2.0	2.2	2.2	2.2	2.2	2.4

A-5 The Walsh Transform for 64 Successive Samples of the Video Signal

1. The First 64 Samples

Walsh no.					
0 → 4	3.05156	2.38594	.26094	.30156	-.24219
5 → 9	-.32031	.28594	.27656	-.27344	-.27031
10 → 14	.27969	.26406	-.24219	-.30156	.27969
15 → 19	.26406	-.05781	-.02969	.04531	.05219
20 → 24	-.03906	-.04844	.04531	.04219	-.05781
25 → 29	-.04844	.05156	.05469	-.03906	-.06719
30 → 34	.05156	.05469	.03594	.03281	-.02969
35 → 39	-.03906	.03594	.03281	-.03594	-.03281
40 → 44	.03594	.03906	-.03594	-.03906	.03594
45 → 49	.03906	-.04219	-.03281	-.04219	-.02656
50 → 54	.03594	.03281	-.02969	-.03906	.02969
55 → 59	.03906	-.04219	-.03281	.04219	.03281
60 → 63	-.02969	-.04531	.03594	.03906	

2. The Second 64 Samples

Walsh no.					
0 → 4	1.58594	-.77031	.79531	-.81094	-.37656
5 → 9	.15469	.12031	.10156	.02344	-.09531
10 → 14	-.12969	.20156	-.14531	.12344	.10156
15 → 19	-.07969	.01719	-.00156	-.07344	.05781
20 → 24	-.00156	.06719	.00781	-.07344	-.02656
25 → 29	-.03281	-.09219	.15156	-.10156	.07969
30 → 34	.04531	-.02344	-.00781	.01094	-.02344
35 → 39	.02031	.02344	.00469	.00781	-.03594
40 → 44	-.05156	.02969	-.01719	.03906	-.00156
45 → 49	-.00781	-.00469	.01406	.01094	-.00781
50 → 54	-.00469	.00156	.04844	-.00781	.02031
55 → 59	-.06094	-.05156	.01719	-.05469	.08906
60 → 63	-.04531	.03594	.00156	.00781	

A-5 (Continued)

3. The Third 64 Samples

Walsh no.

0 → 4	2.55781	.75781	.13281	.72656	-.32031
5 → 9	.14219	-.25781	.21094	.06094	-.02031
10 → 14	-.09531	-.17031	-.14844	-.09219	-.02969
15 → 19	.04531	-.00156	.06094	-.15781	-.05156
20 → 24	-.06094	-.17344	.09531	-.01094	.06406
25 → 29	.00781	-.07344	-.14844	-.12656	-.08281
30 → 34	-.01406	.07344	-.03594	.02031	-.01094
35 → 39	-.02344	.00469	-.03906	-.00781	-.00781
40 → 44	.00469	-.03281	.01094	-.03281	-.03594
45 → 49	.00156	-.02969	.01406	-.04531	.01094
50 → 54	-.06406	.02344	.01406	-.06719	.03281
55 → 59	-.05469	.02031	-.05469	.00781	-.04844
60 → 63	-.05156	.01094	-.03906	.00469	

4. The Fourth 64 Samples

Walsh no.

0 → 4	1.32813	-.57187	-.13750	-.08750	.19375
5 → 9	.14375	.08437	-.17813	.05625	.26875
10 → 14	-.11562	-.15313	.15313	.12812	-.01250
15 → 19	-.25000	.03125	-.04375	-.05312	-.07813
20 → 24	.07188	.07188	-.15625	-.06875	.09062
25 → 29	.05313	-.07500	-.06250	.10000	.05000
30 → 34	-.08437	-.04688	.04688	-.10312	-.03125
35 → 39	.06875	.00625	-.13125	-.01563	.10938
40 → 44	.04375	-.14375	.00938	.07188	-.00313
45 → 49	-.06562	-.05625	.14375	.01250	-.06250
50 → 54	.00312	-.02188	.02187	.03437	-.08125
55 → 59	-.00625	.04063	.00312	-.02500	-.01250
60 → 63	.03125	-.00625	-.02812	-.00313	

A-6 The Walsh Transform for 32 Samples of the Video Signal

1. The First 32 Samples

Walsh no.

0 → 4	5.43750	.56250	-.56250	.56250	-.54375
5 → 9	.54375	-.54375	.54375	-.08750	.08750
10 → 14	-.08750	.08750	-.10625	.10625	-.10625
15 → 19	.10625	.06875	-.06875	.06875	-.06875
20 → 24	.07500	-.07500	.07500	-.07500	-.06875
25 → 29	.06875	-.06875	.06875	-.07500	.07500
30 → 31	-.07500	.07500			

2. The Second 32 Samples

Walsh no.

0 → 4	.66563	.04062	.07813	-.00937	-.00313
5 → 9	-.01562	.05937	-.01563	-.02812	-.00313
10 → 14	.00937	-.00313	-.00938	.00313	.02812
15 → 19	.00312	.00312	-.00938	.00312	.00313
20 → 24	-.00313	-.00313	-.00312	.00938	-.01563
25 → 29	-.00312	.00938	.00937	-.00938	-.00937
30 → 31	.01562	.00313			

3. The Seventh 32 Samples

Walsh no.

0 → 4	.75625	-.22500	.33750	-.09375	.32500
5 → 9	-.26875	.28125	-.26250	-.01250	-.13125
10 → 14	.14375	-.22500	.14375	-.13750	.15000
15 → 19	-.13125	-.05625	.03750	-.12500	.09375
20 → 24	-.10000	.08125	-.06875	.08750	-.05000
25 → 29	-.01875	.05625	-.08750	.04375	-.03750
30 → 31	.02500	-.03125			

4. The Eighth 32 Samples

Walsh no.

0 → 4	1.90000	.05000	.05000	-.26250	-.21250
5 → 9	-.03750	.02500	-.23750	.07500	-.02500
10 → 14	0.00000	.08750	.03750	.01250	.05000
15 → 19	.03750	.15000	.10000	.13750	.12500
20 → 24	.18750	.06250	.06250	.20000	.07500
25 → 29	-.02500	-.01250	.07500	.03750	.01250
30 → 31	.03750	.02500			

APPENDIX B

LAYOUT OF CIRCUIT BOARDS

The following diagrams show the layout of the integrated circuit ships of the two boards of the Walsh function generator and the two boards of the multipliers and summer. Each of the integrated circuits are labelled with the appropriate number used in the schematic diagrams of Figures 12 and 17. The integrated circuit layouts are shown on Figure B-4.

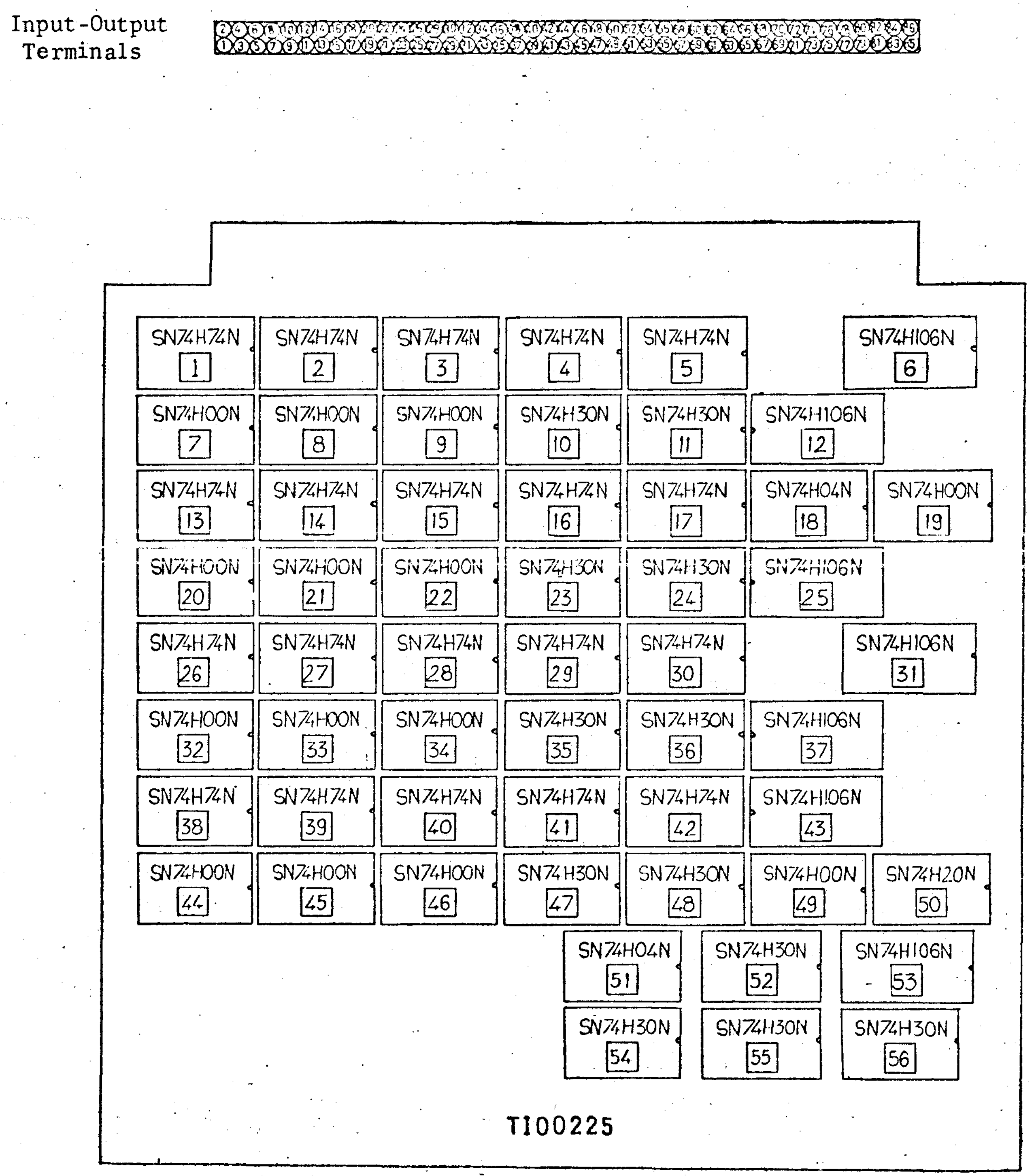

Card Surface Showing Number and Location
of Integrated Circuits

FIGURE B-1 : The Walsh Function Generator Card 1 or Card 2

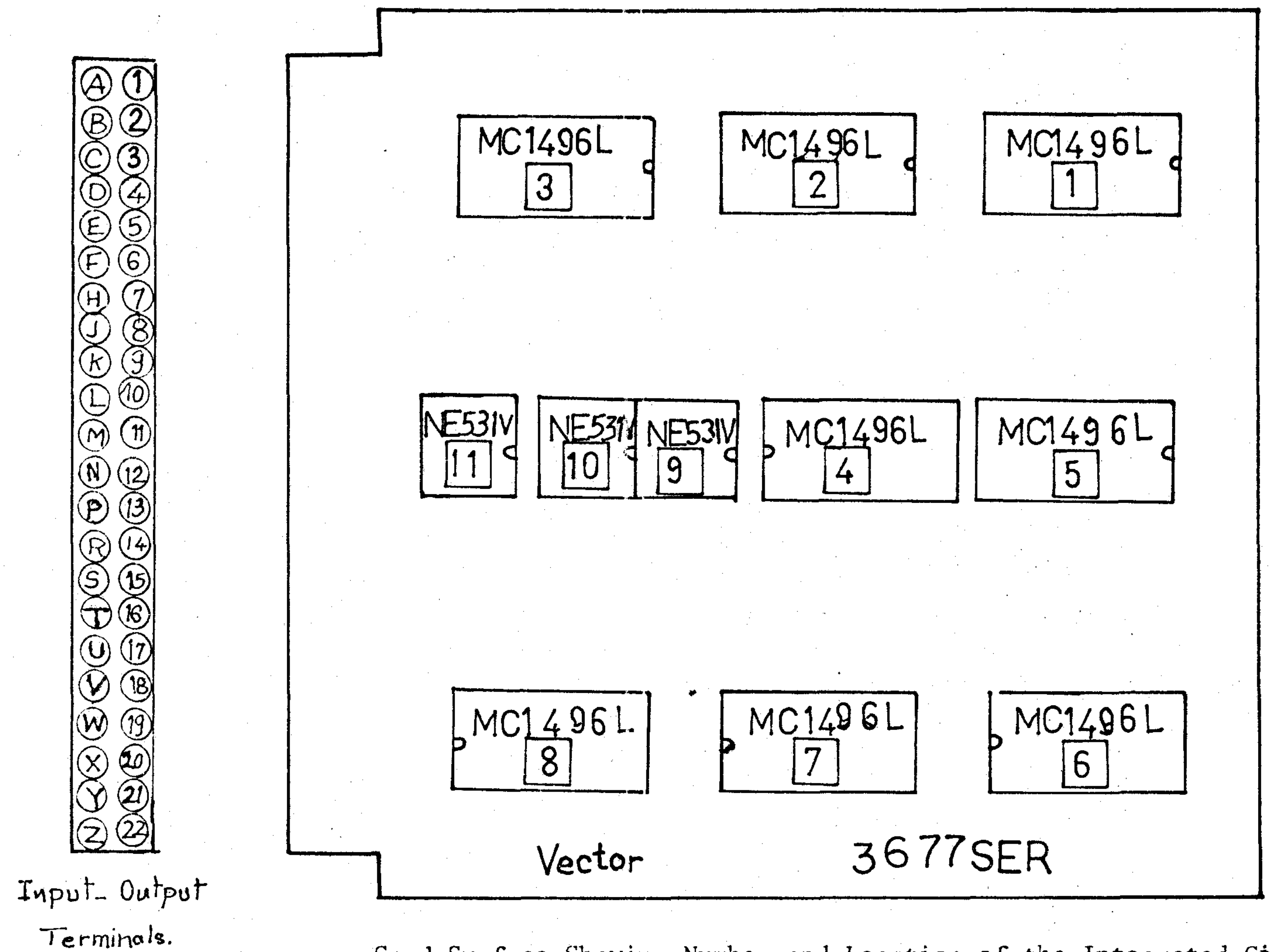

Card Surface Showing Number and Location of the Integrated Circuit

FIGURE B-2: The Multipliers and Summer Card-1

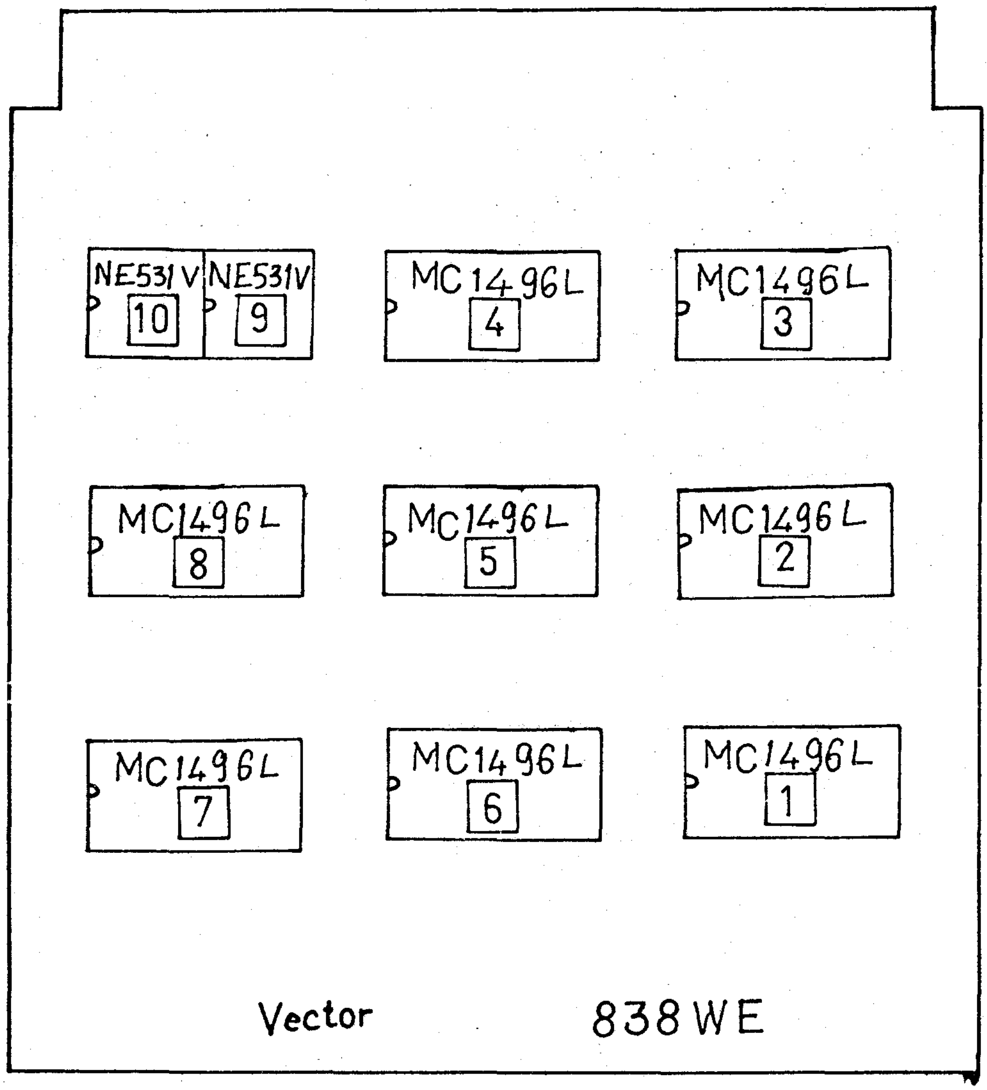

FIGURE B-3: The Multipliers and Summer Card-2 Input-Output Terminals are the Same as in Card-1

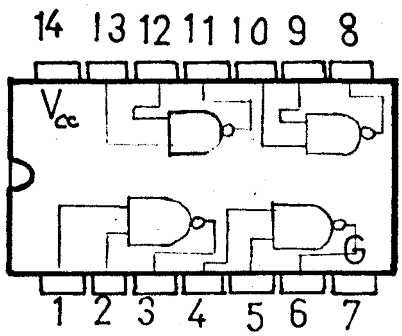

Quadruple 2 input NAND
SN74H00N

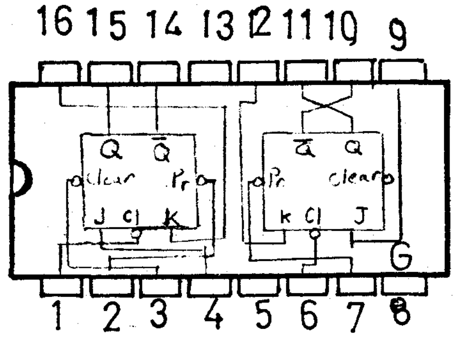

Dual J-K Flip Flop
SN74H106N

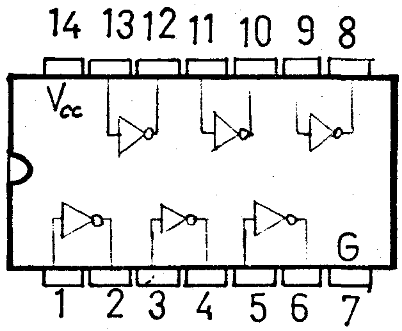

Hex Inverter
SN74H04N

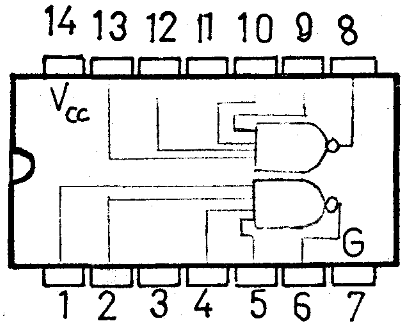

Dual 4 Input NAND
SN74H20N

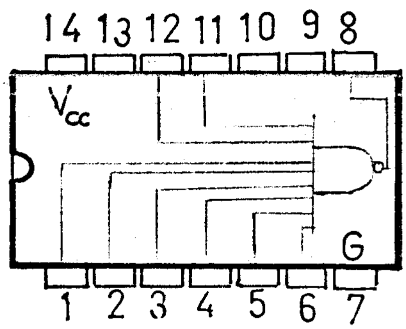

8 Input NAND
SN74H30N

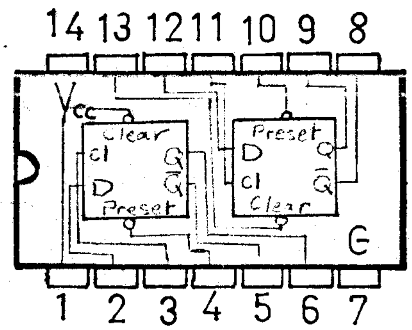

Dual D-type Flip-Flop
SN74H74

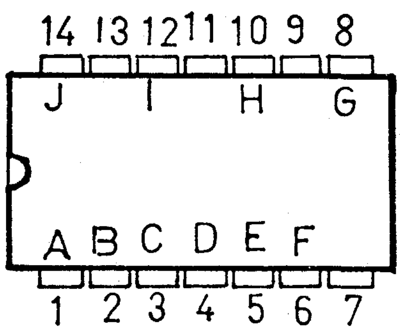

MC1496

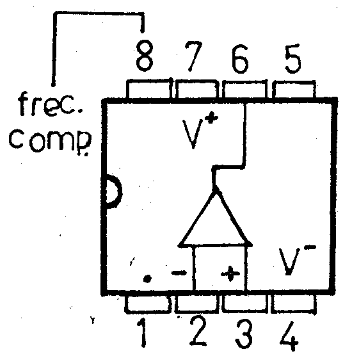

NE531

FIGURE B-4: Integrated Circuit

REFERENCES

[1] Andrews, H. C. and Pratt, W. K., "Digital image transform processing", Symposium on Application of Walsh Function, Naval Research Laboratory, Washington, D.C., March - April 1970.

[2] Brown, W. O. and Elliott, A. R., "A digital instrument for the inverse Walsh transform", Symposium on Application of Walsh Functions, Washington, D.C., March 1972.

[3] Harmuth, H. F., Transmission of Information by Orthogonal Functions, Springer-Verlag, New York/Berlin, 1969.

[4] Henderson, K. W., "Some notes on the Walsh function", IEEE Transactions, Vol. EC-13, pp. 50 - 52, February 1964.

[5] Huang, T. S., Schreiber, W. F., and Tretiak, O. J., "Image processing", Proc. of the IEEE, Vol. 59, No. 11, November 1971.

[6] Kitai, R., and Siemens, K. H., "A hazard-free Walsh function generator", IEEE Trans. on Instrumentation and Measurement, pp. 80 - 83, February 1972.

[7] Shanks, J. L., "Computations of the fast Walsh transform", IEEE Transactions on Computer, May 1969.

[8] Siemens, K. H. and Kitai, R., "Digital Walsh Fourier analysis of periodic waveforms", IEEE Transactions on Instrumentation and Measurement, IB-18, No. 4, December 1969.

[9] Swick, D. A., "Walsh function generation", IEEE Transactions on Information Theory, Vol. IT-15, No. 1, p. 167, January 1969.

[10] Kortman, C. M., "Redundancy reduction. A practical method of data compression", Proc. of IEEE, Vol. 55, No. 3, March 1967.

[11] Andrews, C. A., Davies, J. M., and Schwarz, G. R., "Adaptive data compression", Proc. of IEEE, Vol. 55, No. 3, March 1967.

[12] Elliott, A. R., "A high speed binary rate multiplier", Proc. of IEEE, Vol. 59, No. 8, August 1971.

[13] Phillips, R., "Many digital functions can be generated with a rate multiplier", Electronic Design, No. 3, February 1968.

[14] Fink, Donald G., Television Engineering, McGraw-Hill, 1952.